

See discussions, stats, and author profiles for this publication at: <https://www.researchgate.net/publication/258921673>

Functionalized curcumin analogs as potent modulators of the Wnt/ β -catenin signaling pathway

ARTICLE *in* EUROPEAN JOURNAL OF MEDICINAL CHEMISTRY · NOVEMBER 2013

Impact Factor: 3.45 · DOI: 10.1016/j.ejmech.2013.10.073 · Source: PubMed

CITATIONS

8

READS

58

7 AUTHORS, INCLUDING:



Priti Bahety

National University of Singapore

6 PUBLICATIONS 12 CITATIONS

SEE PROFILE



Chong Yew Lee

Universiti Sains Malaysia

9 PUBLICATIONS 132 CITATIONS

SEE PROFILE



Pui-Lai Rachel Ee

National University of Singapore

42 PUBLICATIONS 1,637 CITATIONS

SEE PROFILE



Original article

Functionalized curcumin analogs as potent modulators of the Wnt/ β -catenin signaling pathway

Pay-Chin Leow, Priti Bahety, Choon Pei Boon, Chong Yew Lee, Kheng Lin Tan, Tianming Yang, Pui-Lai Rachel Ee*

Department of Pharmacy, Faculty of Science, National University of Singapore, 18 Science Drive 4, Singapore 117543, Singapore

ARTICLE INFO

Article history:

Received 26 June 2013

Received in revised form

28 October 2013

Accepted 29 October 2013

Available online 7 November 2013

Keywords:

Curcumin analog

Osteosarcoma

Wnt signaling

Invasion

Drug discovery

ABSTRACT

Osteosarcoma is a primary bone malignancy with aggressive metastatic potential and poor prognosis rates. In our earlier work we have investigated the therapeutic potential of curcumin as an anti-invasive agent in osteosarcoma by its ability to regulate the Wnt/ β -catenin signaling pathway. However, the clinical use of curcumin is limited owing to its low potency and poor pharmacokinetic profile. In this study, an attempt was made to achieve more potent Wnt inhibitory activity in osteosarcoma cells by carrying out synthetic chemical modifications of curcumin. We synthesized a total of five series consisting of 43 curcumin analogs and screened in HEK293T cells for inhibition of β -catenin transcriptional activity. Six promising analogs, which were 6.5- to 60-fold more potent than curcumin in inhibiting Wnt activity, were further assessed for their anti-invasive activity and Wnt inhibitory mechanisms. Western blot analysis showed disruption of β -catenin protein nuclear translocation following treatment with analogs **2f**, **3c** and **4f**. Using transwell assays, we also found that these compounds were more potent than **1a** (curcumin) in impeding the invasion of osteosarcoma cells, possibly through suppressing MMP-9 activity. Structure–activity–relationship studies revealed that Wnt inhibitory effects could be enhanced by shortening and restraining the flexibility of the 7-carbon linker moiety connecting the terminal aromatic rings of curcumin and substituting both rings with appropriate substituents. Our results demonstrate that the synthesized curcumin analogs are more potent Wnt inhibitors in osteosarcoma cell lines as compared to parental curcumin and are good lead compounds for further development. Future *in vivo* tests with these compounds will define their therapeutic potentials as promising drug candidates for clinical treatment of osteosarcoma.

© 2013 Elsevier Masson SAS. All rights reserved.

1. Introduction

Osteosarcoma is an aggressive primary malignancy of the bone resulting from morphologically abnormal osteoblastic cells producing defective immature bone or osteoid. It predominantly affects children and adolescents and shows an aggressive tendency for growth and metastasis, with as many as 20% of patients reported to have developed pulmonary metastasis at the time of diagnosis [1]. Despite the use of various multi-modality regimens of intensive chemotherapy and surgical resection since few decades, prognosis of osteosarcoma patients with pulmonary metastasis is extremely poor with 5-year survival rate of only 10–20% [2]. Moreover, effective therapeutic options are not available for patients with osteosarcoma that relapses following multi-modal first-line treatment or

who suffer from long term toxicities following the standard chemotherapy. These shortcomings have, thus, led to an increase in the efforts invested in understanding the molecular signaling pathways involved in the pathogenesis of the disease with the aim of designing novel, safe and effective therapeutic strategies to help improve clinical outcome among osteosarcoma patients.

With the exact mechanism behind the disease progression and metastasis still remaining uncertain, reports on the contribution of aberrant Wnt/ β -catenin signaling, a key pathway in controlling osteoblast development has come into the limelight in recent osteosarcoma research. In normal circumstances, the pathway is initiated when Wnt ligands bind Frizzled (FZD) and low-density lipoprotein receptor related protein 5/6 (LRP5/6) co-receptors and trigger a cascade of processes, leading to the translocation of β -catenin into the nucleus. In the nucleus, accumulated β -catenin partners with T-cell factor/lymphocyte enhancer factor (Tcf/Lef) family of transcription factors and activates downstream target genes, mainly oncogenes, cell cycle regulators and matrix

* Corresponding author. Tel.: +65 6516 2653; fax: +65 6779 1554.

E-mail address: phaeplr@nus.edu.sg (P.-L.R. Ee).

Table 1
Structure of curcumin analogs (Series 1–5) and their physicochemical properties.

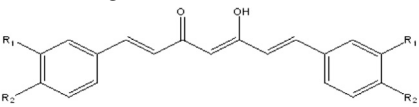
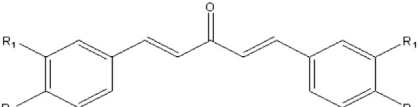
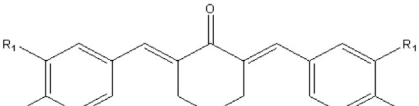
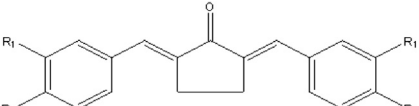
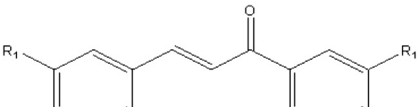
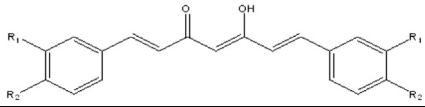
Compound no.	R ₁ (3')	R ₂ (4')	Molecular weight ^a	No. of rotatable bonds ^b	No. of hydrogen bond donors ^b	No. of hydrogen bond acceptors ^b	Clog P ^a
<i>Series 1 analogs</i>							
							
1a (curcumin)	OCH ₃	OH	368.38	7	2	4	2.94
1b	OCH ₃	OCH ₃	396.43	9	0	4	3.89
1c	OH	OCH ₃	368.38	7	2	4	2.94
1d	H	H	276.33	5	0	0	4.58
1e	OCH ₃	H	336.38	7	0	2	4.41
1f	H	OH	308.33	5	2	2	3.24
1g	F	F	348.29	5	0	0	5.01
<i>Series 2 analogs</i>							
							
2a	OCH ₃	OH	326.34	6	2	5	2.64
2b	OCH ₃	OCH ₃	354.40	8	0	5	3.59
2c	OH	OCH ₃	326.34	6	2	5	2.64
2d	H	H	234.39	4	0	1	4.28
2e	OCH ₃	H	294.34	6	0	3	4.11
2f	H	OH	266.29	4	2	3	2.94
2g	F	F	306.25	4	0	1	4.71
<i>Series 3 analogs</i>							
							
3a	OCH ₃	OH	366.41	4	2	5	3.70
3b	OCH ₃	OCH ₃	394.46	6	0	5	4.65
3c	OH	OCH ₃	366.41	4	2	5	3.70
3d	H	H	274.36	2	0	1	5.33
3e	OCH ₃	H	334.41	4	0	3	5.17
3f	H	OH	306.36	2	2	3	4.00
3g	F	F	346.32	2	0	1	5.76
3h	2'F		310.34	2	0	1	5.62
3i	F	H	310.34	2	0	1	5.62
3j	H	F	310.34	2	0	1	5.62
<i>Series 4 analogs</i>							
							
4a	OCH ₃	OH	352.38	4	2	5	3.14
4b	OCH ₃	OCH ₃	380.43	6	0	5	4.09
4c	OH	OCH ₃	352.38	4	2	5	3.14
4d	H	H	260.33	2	0	1	4.77
4e	OCH ₃	H	320.38	4	0	3	4.61
4f	H	OH	292.33	2	2	3	3.44
4g	F	F	332.29	2	0	1	5.20
4h	2'F		296.31	2	0	1	5.06
4i	F	H	296.31	2	0	1	5.06
4j	H	F	296.31	2	0	1	5.06
<i>Series 5 analogs</i>							
							
5a	OCH ₃	OH	300.31	5	2	5	2.50
5b	OCH ₃	OCH ₃	328.36	7	0	5	3.18

Table 1 (continued)

Compound no.	R ₁ (3')	R ₂ (4')	Molecular weight ^a	No. of rotatable bonds ^b	No. of hydrogen bond donors ^b	No. of hydrogen bond acceptors ^b	Clog P ^a
<i>Series 1 analogs</i>							
							
5c	OH	OCH ₃	300.31	5	2	5	2.50
5d	H	H	208.26	3	0	1	3.62
5e	OCH ₃	H	268.31	5	0	3	3.77
5f	H	OH	240.25	3	2	3	2.83
5g	F	F	280.22	3	0	1	4.16

^a Clog P/molecular weight values were determined on ChemDraw Ultra 10.0, CambridgeSoft, Cambridge, MA.

^b No. of rotatable bonds/no. of hydrogen bond donors and acceptors values were determined on MOE, 2009. 10 Chemical Computing Group.

degrading enzymes [3–5]. In osteosarcoma, however, aberrant Wnt/β-catenin activity resulting from β-catenin mutations, increased nuclear β-catenin levels [6,7], over-expression of Wnt ligands [8,9], FZD receptors [9] and LRP5 co-receptor [9–11] have been reported to correlate with metastasis and poorer survival outcome in patients. Through our previous studies, we have demonstrated that forced expression of β-catenin significantly enhanced osteosarcoma cell invasiveness *in vitro* by causing aberrant activation of the pathway [12]. These lines of evidence present Wnt/β-catenin signaling pathway as a potential therapeutic target for treating osteosarcoma.

Over the past few decades, several potential anticancer compounds have been derived from natural products and their constituents, few of which are now either in advanced clinical development or have already been approved for therapeutic use [13]. Curcumin, a dietary phytochemical constituent extracted from the plant turmeric, is one such well-known compound shown to exhibit chemopreventive and chemotherapeutic properties against various types of cancers with a good toxicity profile [14]. The mechanism by which curcumin acts is diverse, but at the molecular level it has been shown to interact with multiple signaling pathways such as nuclear factor-kappa B (NF-κB) [15–18], activator protein (AP)-1 [19,20], signal transducers and activators of transcription (STAT) [18,21–27], Notch signaling [28,29] and Wnt/β-catenin signaling pathway [12,30–32]. However, clinical applications of curcumin are limited mainly due to its low potency, rapid metabolism and low oral bioavailability [33–35]. Synthesizing potent curcumin analogs or developing formulations for its selective delivery are some of the approaches being tried to improve its pharmacological profile and chemotherapeutic potentials [36–41]. In this study, we hypothesized that synthetic chemical modifications of curcumin will yield compounds that combined improved Wnt inhibitory potency with a suitable drug-like character, circumventing the limitations encountered with the parent analog. To this end, we determined the effects of 43 curcumin analogs on the Wnt/β-catenin signaling pathway and identified several promising candidates that were effective in suppressing the activity of the pathway in osteosarcoma. Results from cell invasion assays further demonstrated the potency of these analogs as anti-invasive agents with concomitant reduction in matrix metalloproteinase (MMP)-9 levels. In addition, our structure–activity relationship studies showed that Wnt inhibitory effects were markedly enhanced by shortening and restraining the flexibility of the 7-carbon linker moiety connecting the terminal aromatic rings of curcumin. Our results strongly suggest that curcumin analogs, especially those with the dibenzylidene–cyclohexanone and dibenzylidene–cyclopentanone scaffolds, are promising templates for lead optimization and may yield clinically useful drug candidates for the treatment and prevention of osteosarcoma.

2. Results and discussion

2.1. Rational drug design and synthesis

In this study, our aim was to synthesize more potent curcumin analogs with lower EC₅₀ for Wnt inhibition with limited cell cytotoxicity compared to the parental curcumin. To study the effect of structural modification on Wnt inhibition, we modified the lead compound, curcumin **1-1**, to produce five series of curcumin analogs with diverse linkers joining the terminal phenyl rings as well as different substituents at the phenyl rings. These compounds were synthesized by base-catalyzed Claisen–Schmidt condensation reactions of substituted aromatic aldehydes with the appropriate acetophenones. The structures of curcumin analogs and their physicochemical properties are presented in Table 1. Series 1 consists of curcumin-type compounds that retain the 7-carbon spacer between the terminal phenyl rings known as the diarylheptanoids while Series 2 represents diarylpentanoid analogs with a 5-carbon spacer between the terminal phenyl rings. Series 3 (dibenzylidene–cyclohexanones) and 4 (dibenzylidene–cyclopentanones) consist of diarylpentanoid-type compounds in which flexibility of the 5-carbon chain is constrained by incorporating it as part of a cyclohexanone and cyclopentanone ring, respectively. Lastly, Series 5 compounds, known as chalcones, were considered as structures equivalent to “half a curcuminoid” with loss of symmetry and a shortened linker. The choice of these templates and the associated substitutions at the terminal phenyl rings were prompted by the following observations: Firstly, natural derivatives of curcumin with different substitutions on the end rings were reported to suppress β-catenin/Tcf transcription. Hence, regioisomers of diarylheptanoids (Series 1) were included to determine how changes in substitution pattern would impact inhibitory activity [42]. Secondly, the deletion of the β-ketone moiety in curcumin to give diarylpentanoids (Series 2), dibenzylidene–cyclohexanones (Series 3) and dibenzylidene–cyclopentanones (Series 4) is known to give rise to analogs with improved pharmacological and metabolic profiles [39,43]. Finally, the substitution pattern on the terminal phenyl rings were kept symmetrical (i.e. both rings share the same substitution pattern) and largely restricted to groups present on curcumin. Thus the 3'OCH₃–4'OH substitution pattern of curcumin was modified by (i) excluding either one substituent to give 3'OCH₃ or 4'OH analogs (ii) removing both substituents, (iii) switching their positions to give 3'OH–4'OCH₃ substituted rings; (iv) introducing an additional OCH₃ in place of OH. An exception was the introduction of fluorine which was made in view of the bioisosteric relationship between F and H, as well as the anomalous properties of fluorine which have led to improved activities in many instances [44]. It is noteworthy that all the curcumin analogs have physicochemical properties that comply with the Lipinski's Rule of Five

which provide guidelines for drug-like profiles related to good oral bioavailability (Table 1).

2.2. Evaluation of biological activities

2.2.1. Inhibition of Wnt/ β -catenin signaling activity in HEK293T cells

Owing to their low endogenous levels of β -catenin protein and low β -catenin/Tcf transcriptional activity, HEK293T cells were chosen as a cell model for preliminary screening of Wnt inhibitory activities [45]. Treatment with Wnt-3A CM stimulated Wnt/ β -catenin signaling in HEK293T cells resulting in approximately 30-fold increase in transcriptional activities. Table 2 shows the normalized luciferase activity in the presence of curcumin analogs (1–20 μ M), expressed as % of DMSO with Wnt-3A activation. Compared with control, Wnt-3A CM-induced β -catenin response transcription (CRT) was inhibited by approximately 17.5% and 37.2% with 10 μ M and 20 μ M curcumin treatment, respectively. Given that our lead compound, **1a (curcumin)** was found to have an EC_{50} value of 20.7 ± 0.8 μ M (Table 3), a total of 16 other analogs (Table 2, bold and indicated with #) that were capable of suppressing the Wnt-3A-induced CRT by more than 50% at 20 μ M or lower concentrations (i.e. more potent than curcumin), were shortlisted for subsequent experiments. As shown in Table 3, Series 3 and Series 4 analogs were the most promising, with several members such as **3c**, **f**, **h**, **4c** and **f** having EC_{50} values in the submicromolar ranges. Specifically, the most potent analog from these series, **3c** (EC_{50} 0.3 ± 0.01 μ M) and **4f** (EC_{50} 0.4 ± 0.01 μ M) were approximately 60 and 51 times more potent than parental curcumin in inhibiting Wnt-3A-induced CRT, respectively. Except for **1b**, **3a**, **b**, **4a** and **b**, all the other analogs had limited cytotoxicity at their EC_{50} values (Table 3).

2.2.2. Inhibition of β -catenin/Tcf transcriptional activity in U2OS cells

The effects of selected curcumin analogs **2c**, **3c**, **4c**, **2f**, **3f** and **4f** on the downstream β -catenin/Tcf transcriptional activity were further evaluated in U2OS osteosarcoma cells, which present with activated Wnt/ β -catenin signaling resulting in abnormal accumulation of β -catenin in the nucleus [6]. As shown in Fig. 1, **1a (curcumin)** significantly inhibited β -catenin/Tcf transcriptional activity in U2OS cells by approximately 27.1% and 59.4% at 10 μ M and 20 μ M respectively. In parallel to the results obtained in HEK293T cells, analogs **3c**, **4c**, **2f**, **3f** and **4f** effectively reduced β -catenin/Tcf transcriptional activity in U2OS cells by 25.7–52.7% at 1 μ M concentration, an effect comparable to 10 μ M of parental curcumin. The least potent analog **2c** was also capable of significantly suppressing the transcriptional activity by 49.4% at 5 μ M. In addition, there was no change in the transcriptional activities of the negative control FOPglow plasmid in all instances, indicating the specificity of these compounds for Wnt β -catenin/Tcf transcription.

2.2.3. Effect of curcumin analogs on nuclear translocation of β -catenin

Translocation and accumulation of nuclear β -catenin results in activation of β -catenin/Tcf transcriptional activity [46]. As curcumin disrupts the translocation of β -catenin into the nucleus without changing its total cellular levels [12], we evaluated the effect of curcumin analogs on the cellular levels and localization of β -catenin protein. As shown in Fig. 2, we found that treatments with **2f**, **3c** and **4f** analogs did not alter the amount of β -catenin in the cytoplasm, but caused a reduction in the nuclear fractions at 5 μ M, suggesting a disruption in the translocation of nuclear β -catenin. In contrast, treatment with other analogs (**2c**, **3f** and **4c**) had no effects on either the nuclear or cytoplasmic β -catenin protein levels.

Table 2

Inhibition of Wnt/ β -catenin signaling pathway by curcumin analogs in HEK293T cells.

Compound	Normalized luciferase activity (Firefly/Renilla) ^a			
	Concentration of curcumin analogs			
	1 μ M	5 μ M	10 μ M	20 μ M
<i>Series 1 analogs</i>				
1a (curcumin)	99.4 \pm 3.6	98.2 \pm 3.3	82.5 \pm 7.9	62.8 \pm 12.4
1b[#]	101.6 \pm 3.9	70.0 \pm 1.7	46.5 \pm 7.2	N.D.^b
1c	99.7 \pm 3.1	110.3 \pm 3.1	104.6 \pm 10.3	112.8 \pm 1.1
1d	108.9 \pm 4.4	104.1 \pm 3.4	107.1 \pm 0.8	97.2 \pm 7.5
1e	97.7 \pm 0.9	107.4 \pm 4.0	107.5 \pm 4.2	101.4 \pm 6.1
1f	100.3 \pm 8.3	77.7 \pm 1.8	72.5 \pm 0.6	69.1 \pm 1.9
1g	83.3 \pm 9.0	92.2 \pm 0.5	89.2 \pm 19.2	93.1 \pm 20.0
<i>Series 2 analogs</i>				
2a	118.4 \pm 4.1	110.9 \pm 10.5	110.4 \pm 23.0	90.4 \pm 13.0
2b	107.1 \pm 1.2	107.6 \pm 0.1	108.6 \pm 0.2	103.4 \pm 1.1
2c[#]	82.5 \pm 4.1	38.8 \pm 4.1	34.4 \pm 7.7	N.D.^b
2d	93.0 \pm 2.4	82.7 \pm 9.0	79.7 \pm 14.7	77.9 \pm 17.7
2e	100.4 \pm 5.7	113.9 \pm 3.4	102.7 \pm 2.5	102.9 \pm 4.8
2f[#]	62.3 \pm 2.4	51.3 \pm 6.6	52.0 \pm 5.0	37.8 \pm 3.6
2g	103.0 \pm 13.0	100.0 \pm 12.5	110.1 \pm 6.2	110.9 \pm 9.7
<i>Series 3 analogs</i>				
3a[#]	86.1 \pm 0.8	28.9 \pm 5.6	21.3 \pm 3.8	N.D.^b
3b[#]	97.7 \pm 3.1	64.3 \pm 7.7	62.8 \pm 3.5	40.8 \pm 7.1
3c[#]	37.3 \pm 1.9	27.7 \pm 1.5	24.7 \pm 3.7	21.4 \pm 1.9
3d[#]	85.8 \pm 5.7	49.6 \pm 6.1	40.6 \pm 9.2	39.0 \pm 11.2
3e	93.3 \pm 11.2	60.7 \pm 17.7	72.7 \pm 5.8	81.5 \pm 21.2
3f[#]	51.9 \pm 5.9	26.9 \pm 3.5	26.3 \pm 4.3	16.7 \pm 2.9
3g	94.5 \pm 3.2	125.9 \pm 14.4	117.9 \pm 7.4	113.7 \pm 7.3
3h[#]	52.2 \pm 1.8	21.9 \pm 1.5	14.5 \pm 0.6	20.9 \pm 3.6
3i	96.1 \pm 9.9	119.1 \pm 22.2	105.1 \pm 22.1	103.6 \pm 12.1
3j	70.3 \pm 5.4	65.2 \pm 6.3	61.6 \pm 8.8	60.2 \pm 2.3
<i>Series 4 analogs</i>				
4a[#]	91.6 \pm 5.8	54.1 \pm 4.0	37.5 \pm 2.3	13.3 \pm 2.7
4b[#]	88.9 \pm 2.7	65.9 \pm 6.7	55.5 \pm 6.2	39.2 \pm 7.2
4c[#]	52.6 \pm 6.7	45.0 \pm 5.0	39.5 \pm 4.1	39.2 \pm 5.0
4d[#]	82.7 \pm 4.0	41.5 \pm 5.4	25.3 \pm 6.3	18.4 \pm 2.1
4e	92.3 \pm 3.1	72.7 \pm 2.7	72.0 \pm 5.6	61.3 \pm 9.4
4f[#]	34.3 \pm 1.5	28.3 \pm 3.2	19.6 \pm 3.3	8.0 \pm 2.4
4g	71.0 \pm 7.6	73.1 \pm 6.0	60.2 \pm 2.4	59.5 \pm 6.7
4h	80.0 \pm 12.1	75.7 \pm 12.1	85.3 \pm 5.6	72.8 \pm 4.7
4i	123.8 \pm 16.4	119.2 \pm 5.4	109.0 \pm 10.3	102.6 \pm 7.1
4j	119.5 \pm 10.8	112.5 \pm 15.6	105.4 \pm 6.1	107.7 \pm 5.4
<i>Series 5 analogs</i>				
5a	112.0 \pm 8.3	115.3 \pm 13.9	86.9 \pm 9.7	69.6 \pm 6.7
5b	95.0 \pm 6.5	86.6 \pm 7.7	60.3 \pm 4.3	41.6 \pm 5.5
5c[#]	95.7 \pm 3.9	53.9 \pm 6.9	42.0 \pm 4.7	25.7 \pm 2.8
5d[#]	101.5 \pm 5.7	90.6 \pm 14.1	69.0 \pm 8.8	18.9 \pm 5.4
5e	106.8 \pm 4.3	107.8 \pm 6.4	111.2 \pm 10.5	72.9 \pm 7.0
5f	92.7 \pm 1.7	89.6 \pm 8.7	70.9 \pm 0.4	68.3 \pm 7.0
5g	117.1 \pm 14.8	111.5 \pm 13.3	90.2 \pm 15.7	59.1 \pm 6.8

indicates analogs designated as 'actives' and shortlisted for EC_{50} determinations with an estimated EC_{50} value of less than 20 μ M compared to curcumin (EC_{50} 20.7 ± 0.8).

^a Results are presented as the mean \pm S.E.M of normalized luciferase activity (Firefly/Renilla) from three independent experiments, expressed as % of DMSO (vehicle control) under Wnt-3A induced condition.

^b Not determined (N.D). Tested at 1, 5 and 10 μ M because of toxicity at higher concentrations.

2.2.4. U2OS cell invasion studies

In our previous work, we have shown that curcumin significantly reversed β -catenin plasmid mediated increase in invasive capacity of U2OS cells in a concentration-dependent manner [12]. To determine if curcumin analogs could exert similar, but more potent anti-invasive effects, we performed Matrigel invasion assays [47]. While curcumin treatment significantly reduced the invasive capacity of U2OS cells by $29.0 \pm 5.1\%$ at 5 μ M [12], treatment with analog **2f**, **3c** and **4f** drastically reduced U2OS cell invasiveness by $76.2 \pm 1.4\%$, $81.6 \pm 2.6\%$, and $72.8 \pm 1.0\%$ at the same concentration, respectively (Fig. 3B). We found that these analogs were also

Table 3EC₅₀ values of selected curcumin analogs in HEK293T cells.

Series	Compound	R ₁	R ₂	EC ₅₀ of Wnt inhibition (μM) ^a	Potency (fold) ^b	Cell viability (%) ^c	FOPglow (%) ^c
Series 1	1a (curcumin)	OCH ₃	OH	20.7 ± 0.8	1.0	42.4 ± 2.3	89.3 ± 3.6
	1b	OCH ₃	OCH ₃	8.3 ± 0.2	2.5	41.6 ± 0.1	117.6 ± 17.3
Series 2	2c	OH	OCH ₃	1.8 ± 0.3	11.2	86.6 ± 1.5	105.1 ± 16.0
	2f	H	OH	3.2 ± 0.2	6.5	99.2 ± 6.9	100.4 ± 11.1
Series 3	3a	OCH ₃	OH	2.6 ± 0.2	7.9	57.6 ± 12.4	87.6 ± 7.1
	3b	OCH ₃	OCH ₃	15.9 ± 0.4	1.3	62.1 ± 8.6	103.6 ± 6.4
	3c	OH	OCH ₃	0.3 ± 0.0	59.7	91.6 ± 7.6	93.8 ± 8.3
	3d	H	H	2.0 ± 0.3	10.1	100.0 ± 11.9	90.7 ± 7.1
	3f	H	OH	0.8 ± 0.0	25.8	105.9 ± 10.1	85.1 ± 9.2
	3h[#]	2'F	H	0.9 ± 0.1	22.8	87.0 ± 1.8	93.0 ± 4.5
	4a	OCH ₃	OH	5.9 ± 0.5	3.5	38.4 ± 7.8	90.8 ± 4.8
Series 4	4b	OCH ₃	OCH ₃	17.1 ± 1.8	1.2	40.0 ± 9.5	85.2 ± 5.9
	4c	OH	OCH ₃	0.5 ± 0.0	40.4	86.9 ± 4.5	110.2 ± 12.3
	4d	H	H	3.1 ± 0.4	6.7	83.5 ± 3.3	82.9 ± 7.2
	4f	H	OH	0.4 ± 0.0	50.5	81.4 ± 1.8	101.3 ± 11.3
	5c	OH	OCH ₃	3.9 ± 0.5	5.3	87.2 ± 6.9	130.7 ± 11.7
Series 5	5d	H	H	11.0 ± 1.0	1.9	73.1 ± 12.4	111.9 ± 6.5

Ring substitutions at 2' position.

^a The concentration of curcumin analogs that inhibits 50% of TOPglow β-catenin/Tcf transcriptional activity. EC₅₀ values are presented as the mean ± S.E.M from three independent experiments repeated in triplicate at least.^b Potency fold: EC₅₀ values of curcumin/EC₅₀ values of other analogs.^c Normalized FOPglow transcriptional activities and cell viability of the cells on treatment with analogs at the concentrations of EC₅₀.

effective in suppressing U2OS cell invasion by between $34.8 \pm 2.2\%$ to $71.0 \pm 5.9\%$ at a $1 \mu\text{M}$ concentration. The anti-invasive effects of the analogs were not a result of cell toxicity as no significant growth inhibition was observed at these concentrations (Supplementary data, Fig. S1). In addition, western blot analysis also showed down-regulation in expression of MMP-9 protein at same concentrations (Fig. 3C). Altogether, our results suggest that analogs **2f**, **3c** and **4f** were effective in inhibiting U2OS cell invasiveness at much lower concentrations than curcumin, possibly through down-regulating Wnt target gene, MMP-9.

2.3. Structure activity relationship (SAR)

To have a better understanding of the structural features important for Wnt inhibitory effects, we examined the SAR of the curcumin analogs that were identified to be more potent than parental curcumin in inhibiting Wnt/β-catenin signaling activities in U2OS cells. To study the effect of carbon spacers on SAR, analogs were synthesized with different number of rotatable bonds: Series 3 and 4 (two rotatable bonds), chalcones (three rotatable bonds), Series 2 (four rotatable bonds) and Series 1 (five rotatable bonds). Series 3

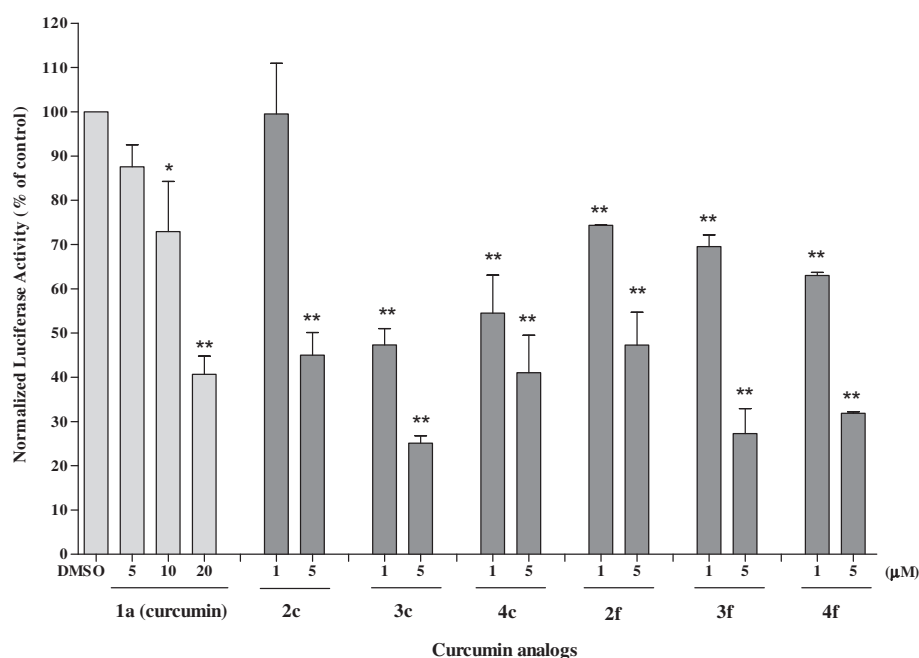


Fig. 1. Effect of curcumin analogs on β-catenin/Tcf transcriptional activity in U2OS cell line. U2OS cells were co-transfected with reporter genes harboring Tcf-4 binding sites (TOPglow) or a mutant Tcf-4 binding site (FOPglow) and pCMV Renilla gene. 20 h post-transfection, U2OS cell were treated with curcumin analogs. 24 h post-treatment firefly luciferase activity was determined and normalized against values for the corresponding Renilla luciferase activity. Results were expressed as the means ± S.E.M of normalized ratios of firefly luciferase and renilla luciferase measurements of three independent experiments. Reporter activity in compound-treated cells is expressed as the percentage of DMSO-treated samples. **p* < 0.05, ***p* < 0.01.

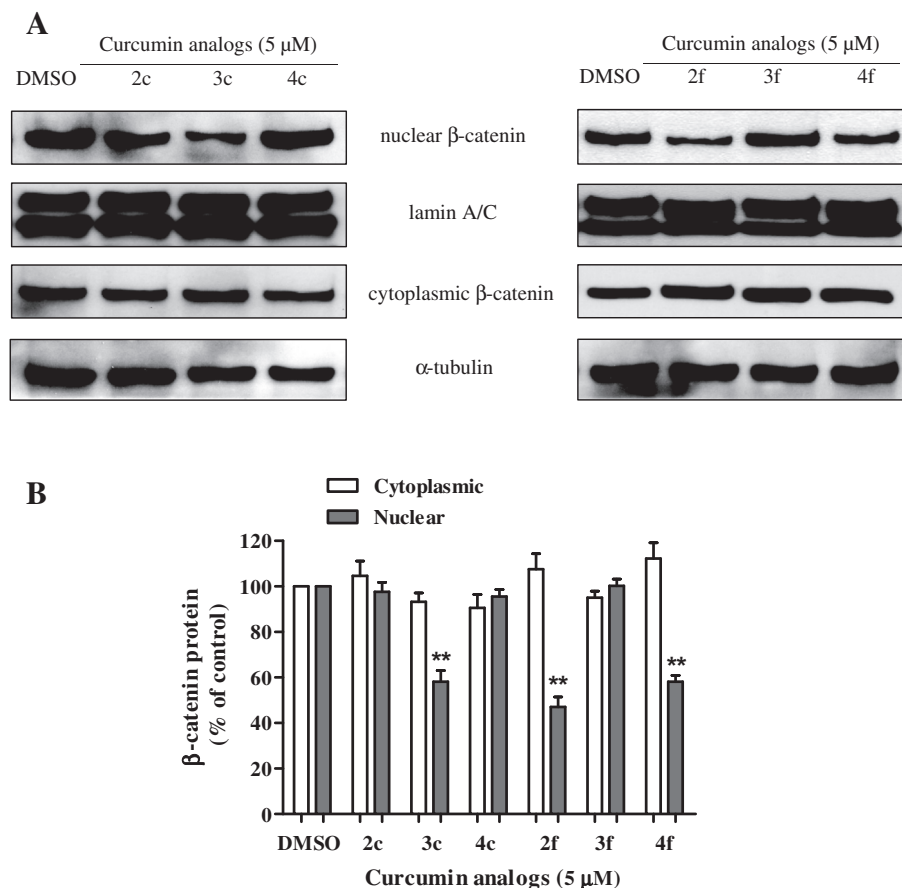


Fig. 2. Effect of curcumin analogs on the cellular and nuclear accumulation of β -catenin. (A) U2OS cells were pre-treated with curcumin analogs at the stated concentrations for 24 h, followed by collection of protein from the cytoplasmic and nuclear fractions. α -tubulin and lamin A/C were used for cytoplasmic and nuclear protein loading controls, respectively. (B) Quantity One software (Bio-Rad, Hercules, CA) was used for quantifying the bands and the results were then expressed relative to the lamin A/C and α -tubulin loading controls. All western blot experiments were repeated at least in triplicates. β -catenin protein expression in compound-treated cells was expressed as the percentage of DMSO-treated samples. * $p < 0.05$, ** $p < 0.01$.

(dibenzylidene-cyclohexanones) and 4 (dibenzylidene-cyclopentanones) analogs, both with conformationally restricted and bulkier tethers between the terminal phenyl rings, exhibited much higher Wnt inhibitory potency than others in which the terminal rings were linked by longer and more flexible carbon spacers (Series 1, 2, 5).

The importance of maintaining 3'-OCH₃–4'-OH substituents at the terminal rings of Series 1–5 compounds was investigated by various permutations centered on the OH/OCH₃ groups. For Series 1 analogs, only the dimethoxy analog **1b** was found to be more potent than curcumin. These results suggested a limited tolerance for the type of groups that can be introduced into phenyl rings of the Series 1 template. A similar trend was observed in Series 2 and 5 where no more than 2 different substitution patterns were permissible, with the preferred substituents being 3'-OH–4'-OCH₃ and not dimethoxy as noted for Series 1. On the other hand, the Wnt inhibitory activities of Series 3 and 4 were less influenced by the type of substituents on the terminal phenyl rings. In addition, all non-fluorinated cyclic analogs from both series, except those with 3'-methoxy ring substituent (**3e** and **4e**) were found to be more potent than curcumin. Interestingly, compound **3h**, which was mono-fluorinated at the 2' position, was found to be active, with luciferase activity reduced to approximately 45.7% and 15% at 5 μ M and 10 μ M concentrations, respectively. This trend was however not seen for compound **4h** in Series 4 or among other fluorinated analogs (4'-F or 3', 4'-diF) represented across the

different series. Overall, the influence of the nature of ring substituent on the Wnt inhibitory activities may be broadly ranked in the sequence: 3'-OH–4'-OCH₃ \approx 4'-OH (most active) \gg 3'-H–4'-H $>$ 3'-OCH₃ 4'-OH $>$ 3'-OCH₃–4'-OCH₃ \gg 3'-OCH₃ \approx 4'-F \approx 4'-F (least active).

The poor activity of the 3'OCH₃ analogs in all the series suggested the need to restrain the steric dimensions of the groups at this position. It also reflected a preference for groups that were not electron withdrawing at this position. It was notable that 3'OCH₃ was electron withdrawing unlike 4'OCH₃ which was electron donating, as seen from their Hammett sigma values (σ_p OCH₃ –0.27; σ_m OCH₃ = 0.12). Inhibitory activity may be determined by interplay of the size and electrostatic nature of groups at this position. Thus, the poor activity of 3'F analogs would suggest that the strong electron withdrawing effect of F has more than offset its small steric dimensions while the moderate activities of analogs with unsubstituted phenyl rings (**3d**, **4d**) may be attributed to their limited size requirements. From these results, it is tempting to suggest that Wnt inhibitory activity is favored by the absence of electron withdrawing groups on the terminal phenyl rings of Series 3 and 4. Support for this view was seen from the exceptionally good activities of the 4'OH analogs (**3f**, **4f**) and the 3'OH–4'OCH₃ analogs (**3c**, **4c**). As to why switching OH/OCH₃ to 3'OCH₃–4'OH resulted in analogs (**3a**, **4a**) with a modest decline in activity, may be attributed to the location of the bulkier OCH₃ at the 3' position. Taken together, some general SAR trends were deduced from the results

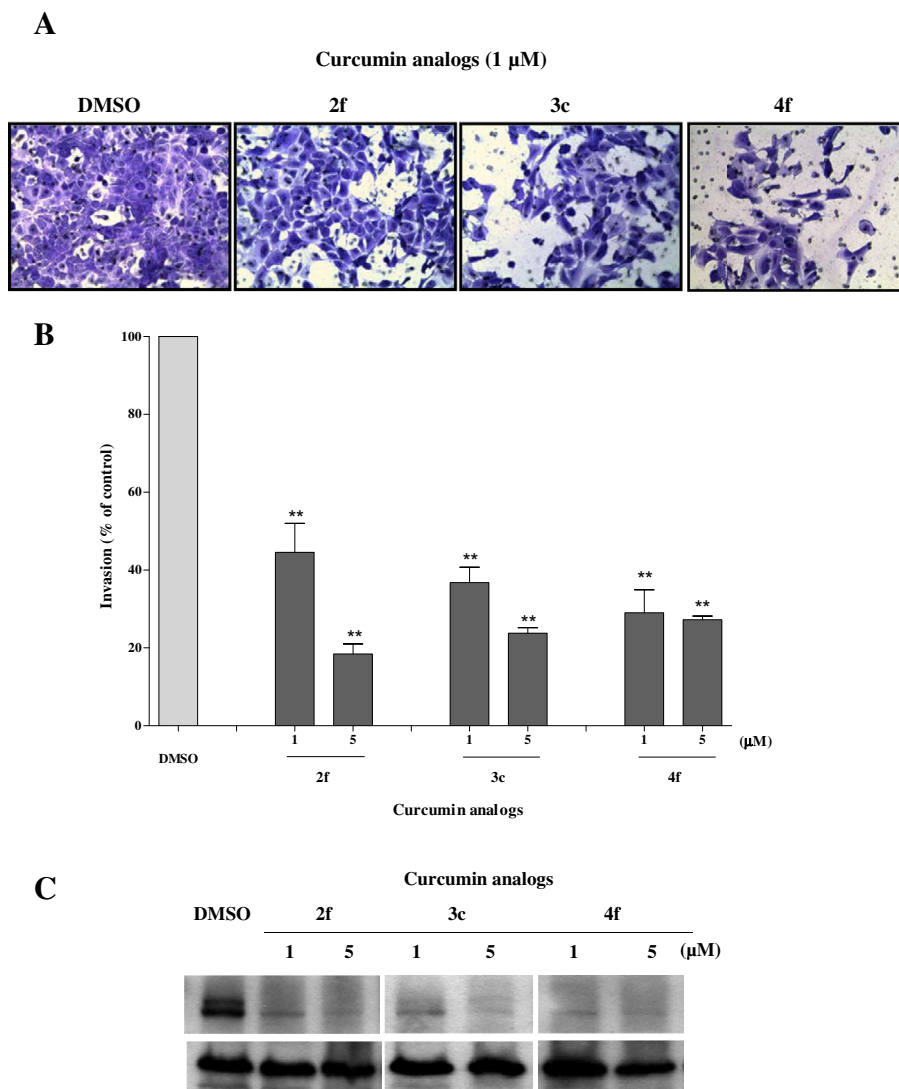


Fig. 3. Effect of curcumin analogs on U2OS cell invasion. (A) U2OS cells were pre-treated with curcumin analogs for 24 h before they were seeded into Matrigel-coated inserts. Cells that invaded to the lower surface of the insert were captured with a light microscope at 200 \times magnification after staining with crystal violet dye. Images were representations from three independent experiments. (B) Ten random fields were counted for the number of invaded U2OS cells. Cell invasion data was presented as means \pm S.E.M of three independent experiments. Cell invasion in compound-treated cells was expressed as the percentage of DMSO-treated samples, * p < 0.05, ** p < 0.01. (C) U2OS cells were treated with indicated concentrations of curcumin analogs or DMSO (vehicle control) for 24 h before proteins were collected for western blot. The blots shown were representative of three independent experiments. α -tubulin was used as a loading control.

obtained and were summarized in Fig. 4. These requirements may reflect the involvement of these groups in key interactions with target proteins and would require further confirmation with additional analogs.

3. Conclusion

Our study identified three new curcumin analogs that were more potent than parent curcumin as effective Wnt inhibitors and anti-invasive agents in human osteosarcoma. SAR studies revealed that the Wnt inhibitory effects could be markedly enhanced by introducing conformational restriction in the central linker and appropriate ring substituents such as a strong electron donating group at the 4' ring position. These SAR trends observed may reflect the involvement of these groups in key interactions with the target proteins. Our results strongly suggest that curcumin analogs especially those with the dibenzylidene-cyclohexanones and dibenzylidene-cyclopentanones templates are promising scaffolds for future structural optimization and are promising candidate

drugs for further development as chemotherapeutic agents for the treatment and prevention of osteosarcoma.

4. Experimental protocols

4.1. Chemistry

4.1.1. General experimental details for synthesis

Reagents (synthetic grade or better) were obtained from Sigma–Aldrich Chemical Company Inc (Singapore) and used without further purification. Melting points were determined in open capillary tubes on a Gallenkamp melting point apparatus and reported as uncorrected values. Mass spectra were captured on an LCQ Finnigan MAT equipped with an Atmospheric Chemical Ionization (APCI) probe and m/z ratios for the molecular ions ($M + 1$)⁺ were reported. Chemical shifts of ¹H NMR and ¹³C NMR spectra, obtained on a Bruker Spectrospin 300 Ultrashield spectrometer at 300 MHz and 75 MHz respectively, were analyzed using MestRec-C 4.9.9.6 (Mestrelab Research SL, Spain) and reported in δ (ppm)

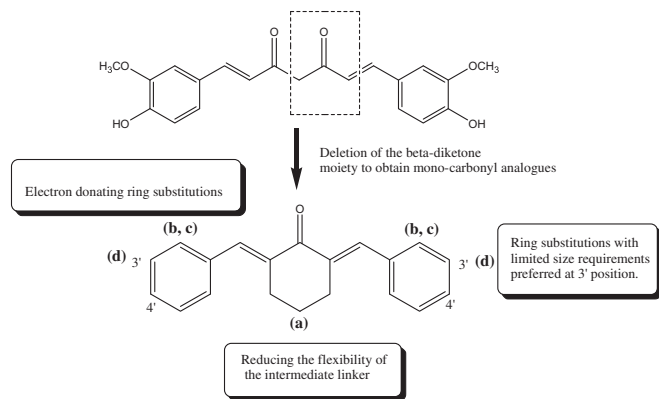


Fig. 4. Structural features of curcumin analogs important for enhanced Wnt inhibitory activity. (a) Reducing the flexibility of the intermediate linker joining the terminal phenyl rings improved Wnt inhibitory activity. Incorporating the linker as part of a ring structure such as dibenzylidene-cyclohexanone (Series 3) and dibenzylidene-cyclopentanone (Series 4) spacers are favored. (b) Flexibility of the intermediate side chain influenced the substitution on the terminal phenyl rings. Only limited ring substitution patterns were tolerated in analogs with flexible linkers (Series 1, 2, 5), but a wider range of substitution patterns were permitted in analogs that had less flexible linkers (Series 3, 4). (c) Electron donating ring substitutions are more favorable. (d) Ring substitutions with limited size requirements are preferred at the 3' position.

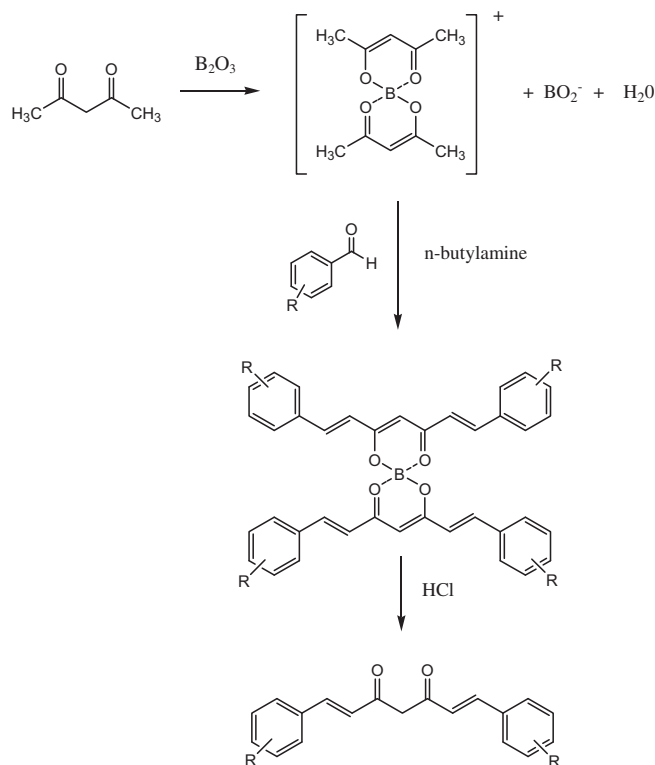
relative to tetramethylsilane (TMS) as an internal standard. Silica 60 F254 sheets (Merck, Darmstadt, Germany) and silica gel 60 (0.040–0.063) (Merck, Darmstadt, Germany) were used for Thin Layer Chromatography (TLC) and flash chromatography respectively. Purity of the final compounds were verified either by combustion analysis (C, H) on a Perkin Elmer PRE-2400 Elemental Analyzer or by High Pressure Liquid Chromatography (HPLC) using two different solvent systems. Spectroscopic data, melting points, yields and purities of individual compounds were reported.

4.1.2. General procedure for the synthesis of Series 1 curcumin analogs

Curcumin analogs from Series 1 were prepared according to Pedersen method with slight modifications [48] (Scheme 1). A mixture of boric anhydride (0.35 g, 5 mmol), suspended in ethyl acetate (EtOAc), and acetylacetone (1.00 g, 10 mmol) was first stirred for 3 h at 70 °C. After removing the solvent, the resultant white residue was washed with hexane. Following this, substituted aldehyde (20 mmol), tributyl borate (4.60 g, 20 mmol) and 20 mL EtOAc were added and stirred at room temperature for a further 30 min. Butylamine (73 mg, 1 mmol) dissolved in EtOAc (5 mL) was then added dropwise over 15 min and the mixture was stirred at 70 °C for another 24 h. Next, the reaction mixture was heating for 30 min at 60 °C after adjusting to pH5 by adding 1 N HCl. EtOAc (3 × 50 mL) was then used to extract the crude product from the water layer. The organic layer was washed with brine, dried with anhydrous NaSO₄ and evaporated *in vacuo* to give either a solid or liquid residue and purified by column chromatography on silica gel using hexane:ethyl acetate as eluting solvents. Further purification by re-crystallization from ethyl acetate yielded yellow crystals.

4.1.3. General procedure for the synthesis of Series 2, 3, 4 and 5 alkoxyated curcumin

The method by Liang et al. was followed [49] (Scheme 2). To a solution of substituted benzaldehyde (30 mmol) in methanol (20 mL) was added appropriately substituted ketone (15 mmol) such as acetone (Series 2), cyclohexanone (Series 3) and cyclopentanone (Series 4). For the synthesis of Series 5 analogs, 15 mmol of substituted benzaldehyde and 15 mmol of substituted ketone were

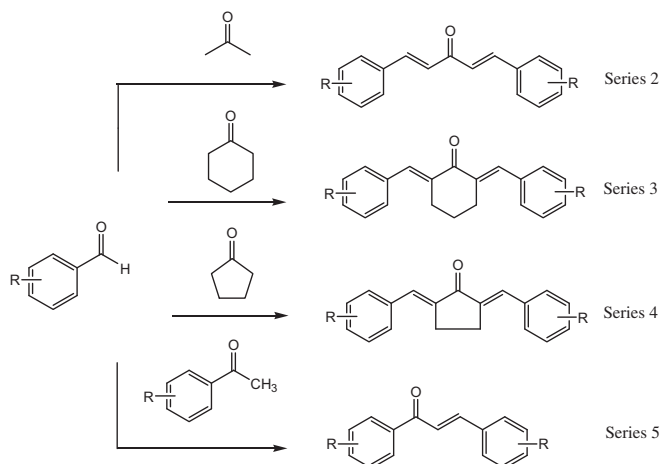


Scheme 1. General method for the synthesis of Series 1 curcumin analogs.

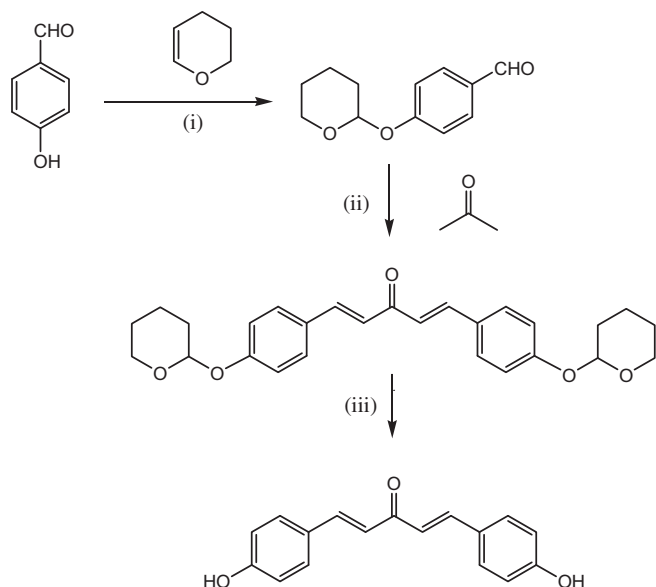
used instead. The resultant mixture was stirred at room temperature for 20 min before 20% (w/v) NaOH (3.0 mL, 15 mmol) was added dropwise. After the reaction has completed, the residue was poured into saturated NH₄Cl solution and filtered. The precipitate was washed with brine and cold ethanol, dried with anhydrous NaSO₄, evaporated *in vacuo* to give either a solid or liquid residue and purified by column chromatography on silica gel using hexane:ethyl acetate as eluting solvents. Further purification by re-crystallization from ethyl acetate or ethanol yielded yellow crystals.

4.1.4. General procedure for the synthesis of Series 2, 3 and 4 hydroxylated curcumin analogs

For compounds with phenolic hydroxyl substituent, additional protection and de-protection of the phenolic hydroxyl groups on the benzaldehyde were required and the method by Liang et al. was



Scheme 2. General synthesis of curcumin analogs from Series 2, 3, 4 and 5.



Scheme 3. Protection and deprotection of phenolic hydroxyl groups for the synthesis of compound **2f**. Reagents and conditions: (i) pyridinium *p*-toluenesulfonate, RT, 4 h (ii) 20% NaOH, RT, 3 h. (iii) 4 M HCl, RT, 4 h.

followed [49] (Scheme 3). A solution of 3,4-dihydro- α -pyran (44 mmol) in dichloromethane (40 mL) was added dropwise to a well stirred suspension of hydroxyl benzaldehyde (28.8 mmol) and pyridinium *p*-toluenesulfonate (0.32 mmol) in dichloromethane (80 mL) and stirred at room temperature for 4 h. The reaction mixture was then washed with 1 M NaCO₃ solution (60 mL \times 3) and brine (60 mL \times 3), dried with anhydrous NaSO₄, evaporated *in vacuo* and purified by column chromatography on silica gel using hexane:ethyl acetate as eluting solvents to yield 4-(tetrahydropyran-2-yloxy) as a pale yellow oil. This purified protected derivative was condensed with substituted ketone at a ratio of 2:1 using similar procedures as described earlier for alkoxyated curcumin analogs. At the end of the reaction, the protecting groups were removed by acidifying with 4 M HCl, followed by stirring the mixture for 4 h at room temperature. The reaction mixture was then diluted with water, followed by extracting with ethyl acetate (50 mL \times 3) and the combined organic phase was washed with brine (50 mL \times 3), dried over anhydrous NaSO₄, evaporated *in vacuo* and purified by column chromatography and/or re-crystallization as described earlier.

4.1.5. General procedure for the synthesis of Series 5 hydroxylated chalcones

For chalcones with phenolic hydroxyl substituent, additional protection and de-protection of the phenolic hydroxyl groups on both the acetophenone and substituted aromatic aldehyde were required. The benzaldehyde (15 mmol) and aromatic ketone (15 mmol), were reacted separately each with pyridinium *p*-toluenesulfonate (1 mmol) and 3,4-dihydro-2H-pyran (40 mmol) in dichloromethane (40 mL) and stirred at room temperature for 4 h. The reaction mixture was then washed with 1 M NaCO₃ solution (60 mL \times 3) and brine (60 mL \times 3), dried with anhydrous NaSO₄, evaporated *in vacuo* to yield the crude tetrahydropyranyl ether as a pale yellow oil and used without purification. This crude protected aromatic aldehyde and ketones was then reacted at a ratio of 1:1 using similar procedures as described earlier for alkoxyated Series 5 analogs. At the end of the reaction, the protecting groups were removed by acidifying with 4 M HCl, followed by stirring the mixture for 4 h at room temperature. The reaction mixture was then diluted

with water, followed by extracting with ethyl acetate (50 mL \times 3) and the combined organic phase was washed with brine (50 mL \times 3), dried over anhydrous NaSO₄, evaporated *in vacuo* and purified by column chromatography and/or re-crystallization as described earlier.

4.1.6. Characterization of synthesized compounds

4.1.6.1. Compound 1a (curcumin). IUPAC name: 5-hydroxy-1,7-bis (4-hydroxy-3-methoxy phenyl) hepta-1,4,6-trien-3-one. Yellow–orange crystals. C₂₁H₂₀O₆. Melting point: 183 °C. ¹H NMR (300 MHz, CDCl₃) δ : 3.95 (6H, s, OCH₃ \times 2), 5.80 (1H, s, COCH=C), 6.48 (2H, d, *J* = 16 Hz, CHCO \times 2), 6.93 (2H, d, *J* = 8 Hz, Ar–H), 7.05 (2H, s, Ar–H), 7.12 (2H, d, *J* = 8 Hz, Ar–H), 7.59 (2H, d, *J* = 16 Hz, Ar–CH=C \times 2). ¹³C NMR (75 MHz, CDCl₃) δ : 55.928, 101.089, 109.626, 114.800, 121.769, 122.828, 127.677, 140.491, 140.491, 146.755, 147.823, 151.915, 183.229. MS (APCI) *m/z*: 369.0 (*M* + 1)⁺. Anal calcd for C₁₇H₁₄O₅: C, 68.45; H, 4.73; Found: C, 68.03; H, 4.78.

4.1.6.2. Compound 1b. IUPAC name: 5-hydroxy-1,7-bis (3,4-dimethoxy phenyl) hepta-1,4,6-trien-3-one. Orange powder. C₂₃H₂₄O₆. Yield: 39.0%. Melting point: 130–131 °C. ¹H NMR (300 MHz, CDCl₃) δ : 3.92 (6H, s, OCH₃ \times 2), 3.93 (6H, s, OCH₃ \times 2), 5.82 (1H, s, COCH=C), 6.50 (2H, d, *J* = 16 Hz, CHCO \times 2), 6.88 (2H, d, *J* = 8 Hz, Ar–H), 7.10 (4H, m, Ar–H), 7.61 (2H, d, *J* = 16 Hz, Ar–CH=C \times 2). ¹³C NMR (75 MHz, CDCl₃) δ : 55.843, 55.912, 76.642, 77.066, 77.490, 101.274, 109.754, 111.096, 121.967, 122.578, 128.002, 140.334, 149.173, 150.992, 183.204. MS (APCI) *m/z*: 396.9 (*M* + 1)⁺. HPLC (MeOH:H₂O = 80:20) *t*_R (min): 9.394. *P*_{HPLC}/%: 97.50. HPLC (ACN:H₂O = 80:20) *t*_R (min): 2.931. *P*_{HPLC}/%: 100.00.

4.1.6.3. Compound 1c. IUPAC name: 5-hydroxy-1,7-bis (3-hydroxy-4-methoxy phenyl) hepta-1,4,6-trien-3-one. Orange powder. C₂₁H₂₀O₆. Yield: 35.0%. Melting point: 192 °C. ¹H NMR (300 MHz, CDCl₃) δ : 3.92 (6H, s, OCH₃ \times 2), 5.82 (1H, s, COCH=C), 6.48 (2H, d, *J* = 16 Hz, CHCO \times 2), 6.87 (2H, d, *J* = 8 Hz, Ar–H), 7.04 (2H, d, *J* = 8 Hz, Ar–H), 7.15 (2H, s, Ar–H), 7.53 (2H, d, *J* = 16 Hz, Ar–CH=C \times 2). MS (APCI) *m/z*: 369.0 (*M* + 1)⁺. HPLC (MeOH:H₂O = 80:20) *t*_R (min): 2.450. *P*_{HPLC}/%: 95.97. HPLC (ACN:H₂O = 80:20) *t*_R (min): 1.849. *P*_{HPLC}/%: 95.48.

4.1.6.4. Compound 1d. IUPAC name: 5-hydroxy-1,7-diphenyl hepta-1,4,6-trien-3-one. Yellow powder. C₁₉H₁₆O₂. Yield: 50.0%. Melting point: 138–140 °C. ¹H NMR (400 MHz, CDCl₃) δ : 7.68 (2H, d, *J* = 16 Hz), 7.57–7.55 (4H, m), 7.40–7.39 (6H, m), 6.64 (2H, d, *J* = 15.6 Hz), 5.86 (1H, s). ¹³C NMR (100 MHz, CDCl₃) δ : 101.752, 124.194, 128.237, 128.878, 130.200, 134.551, 140.264, 183.092. MS (APCI) *m/z*: 277.0 (*M* + 1)⁺. HPLC (MeOH:H₂O = 80:20) *t*_R (min): 9.281. *P*_{HPLC}/%: 99.86. HPLC (ACN:H₂O = 70:30) *t*_R (min): 12.003. *P*_{HPLC}/%: 98.50.

4.1.6.5. Compound 1e. IUPAC name: 5-hydroxy-1,7-bis (3-methoxy phenyl) hepta-1,4,6-trien-3-one. Brownish-orange powder. C₂₃H₂₄O₄. Yield: 40.0%. Melting point: 59–60 °C. ¹H NMR (300 MHz, CDCl₃) δ : 3.85 (6H, s, OCH₃ \times 2), 5.86 (1H, s, COCH=C), 6.62 (2H, d, *J* = 16 Hz, –CHCO– \times 2), 6.88 (2H, d, *J* = 2 Hz, Ar–H), 6.95 (2H, d, *J* = 10 Hz, Ar–H), 7.08 (2H, s, Ar–H), 7.30 (2H, s, Ar–H), 7.633 (2H, d, *J* = 16 Hz, Ar–CH=C \times 2). ¹³C NMR (75 MHz, CDCl₃) δ : 55.289, 101.794, 113.037, 115.908, 120.794, 124.328, 129.882, 136.329, 140.543, 159.889, 183.230. MS (APCI) *m/z*: 337.0 (*M* + 1)⁺. HPLC (MeOH:H₂O = 80:20) *t*_R (min): 1.784. *P*_{HPLC}/%: 95.81. HPLC (ACN:H₂O = 80:20) *t*_R (min): 1.608. *P*_{HPLC}/%: 97.30.

4.1.6.6. Compound 1f. IUPAC name: 5-hydroxy-1,7-bis (4-hydroxy phenyl) hepta-1,4,6-trien-3-one. Orange–red crystals. C₁₉H₁₆O₆. Yield: 49.0%. Melting point: 229–230 °C. ¹H NMR (400 MHz,

DMSO- d_6) δ : 10.10 (2H, s), 7.57–7.52 (6H, m), 6.82 (4H, d, J = 8.8 Hz), 6.68 (2H, d, J = 15.6 Hz), 6.04 (1H, s). ^{13}C NMR (100 MHz, DMSO- d_6) δ : 100.93, 115.92, 120.891, 125.979, 130.464, 140.522, 159.893, 183.325. MS (APCI) m/z : 369.0 ($M + 1$) $^+$. HPLC (MeOH:H₂O = 80:20) t_R (min): 5.055. $P_{\text{HPLC}}/\%$: 96.85. HPLC (ACN:H₂O = 80:20) t_R (min): 1.670. $P_{\text{HPLC}}/\%$: 99.14.

4.1.6.7. Compound 1g. IUPAC name: 1,7-bis (3,4-difluoro phenyl)-5-hydroxy hepta-1,4,6-trien-3-one. Yellow powder. C₁₉H₁₂F₄O. Yield: 94.0%. Melting point: 229–230 °C. ^1H NMR (300 MHz, DMSO- d_6) δ : 5.82 (1H, s, COCH=C), 6.53 (2H, J = 16 Hz, –CHCO– \times 2), 7.14–7.41 (m, 7H, Ar–H + Ar–CH=C \times 2), 7.57 (2H, d, 8 Hz, Ar–H). ^{13}C NMR (75 MHz, DMSO- d_6) δ : 76.5764, 77.0000, 77.2022, 77.4236, 78.3575, 102.1870, 116.0418, 117.7460, 117.9771, 124.8419, 132.1689, 138.4753, 182.7933. MS (APCI) m/z : 309.2 ($M + 1$) $^+$. HPLC (MeOH:H₂O = 80:20) t_R (min): 14.846. $P_{\text{HPLC}}/\%$: 99.85. HPLC (ACN:H₂O = 70:30) t_R (min): 2.198. $P_{\text{HPLC}}/\%$: 98.68.

4.1.6.8. Compound 2a. IUPAC name: 1,5-bis (4-hydroxy-3-methoxy phenyl) penta-1,4-dien-3-one. Greenish-yellow powder. C₁₉H₁₈O₅. Yield: 33.0%. Melting point: 106 °C. ^1H NMR (300 MHz, CDCl₃) δ : 3.96 (6H, s, OCH₃ \times 2), 6.90–6.95 (4H, m, Ar–H + COCH=C \times 2), 7.09–7.17 (m, 4H, Ar–H), 7.68 (2H, d, J = 16 Hz, Ar–CH=C \times 2). ^{13}C NMR (75 MHz, DMSO- d_6) δ : 55.689, 111.350, 115.632, 122.965, 123.334, 126.306, 142.754, 149.942, 188.015. MS (APCI) m/z : 326.9 ($M + 1$) $^+$. HPLC (MeOH:H₂O = 80:20) t_R (min): 1.794. $P_{\text{HPLC}}/\%$: 95.81. HPLC (ACN:H₂O = 70:30) t_R (min): 1.608. $P_{\text{HPLC}}/\%$: 97.40.

4.1.6.9. Compound 2b. IUPAC name: 1,5-bis (3,4-dimethoxy phenyl) penta-1,4-dien-3-one. Orange–yellow solid. C₂₁H₂₂O₅. Yield: 52.0%. Melting point: 93–95 °C. ^1H NMR (300 MHz, CDCl₃) δ : 3.93 (6H, s, OCH₃ \times 2), 3.95 (6H, s, OCH₃ \times 2), 6.89 (2H, d, J = 8.1 Hz, Ar–H), 6.96 (d, J = 16 Hz, COCH=C \times 2), 7.14–7.21 (m, 4H, Ar–H), 7.69 (d, J = 16 Hz, Ar–CH=C \times 2). ^{13}C NMR (75 MHz, CDCl₃) δ : 55.845, 55.892, 109.840, 111.035, 123.033, 123.530, 127.763, 142.984, 149.156, 151.252, 188.629. MS (APCI) m/z : 355.0 ($M + 1$) $^+$. HPLC (MeOH:H₂O = 80:20) t_R (min): 3.129. $P_{\text{HPLC}}/\%$: 95.49. HPLC (ACN:H₂O = 70:30) t_R (min): 2.762. $P_{\text{HPLC}}/\%$: 94.59.

4.1.6.10. Compound 2c. IUPAC name: 1,5-bis (3-hydroxy-4-methoxy phenyl) penta-1,4-dien-3-one. Yellow powder. C₁₉H₁₈O₅. Yield: 33.27%. Melting point: 189–190 °C. ^1H NMR (300 MHz, DMSO- d_6) δ : 3.77 (s, 6H, OCH₃ \times 2), 6.93 (d, 2H, J = 8 Hz, Ar–H), 7.03 (d, J = 16 Hz, COCH=C \times 2), 7.14–7.17 (m, 4H, Ar–H), 7.57 (d, J = 16 Hz, 2H, Ar–CH=C \times 2). ^{13}C NMR (75 MHz, DMSO- d_6) δ : 56.0, 112.592, 114.706, 122.818, 123.919, 128.057, 143.757, 147.087, 150.906, 189.454. MS (APCI) m/z : 327.0 ($M + 1$) $^+$. HPLC (MeOH:H₂O = 80:20) t_R (min): 3.129. $P_{\text{HPLC}}/\%$: 95.49. HPLC (ACN:H₂O = 70:30) t_R (min): 2.762. $P_{\text{HPLC}}/\%$: 94.59.

4.1.6.11. Compound 2d. IUPAC name: 1,5-diphenyl penta-1,4-dien-3-one. Yellow crystals. C₁₇H₁₄O. Yield: 28.3%. Melting point: 113 °C. ^1H NMR (400 MHz, CDCl₃) δ : 7.75 (2H, d, J = 16 Hz), 7.63–7.61 (4H, m), 7.42–7.41 (6H, m), 7.09 (2H, d, J = 17.3 Hz). ^{13}C NMR (100 MHz, CDCl₃) δ : 125.327, 128.310, 128.872, 130.411, 134.964, 143.206, 188.805. MS (APCI) m/z : 235.3 ($M + 1$) $^+$. $P_{\text{HPLC}}/\%$: 95.37. HPLC (ACN:H₂O = 80:20) t_R (min): 3.075. $P_{\text{HPLC}}/\%$: 99.72.

4.1.6.12. Compound 2e. IUPAC name: 1,5-bis (3-methoxyphenyl) penta-1,4-dien-3-one. Yellow solid. C₁₉H₁₈O₃. Yield: 45.7%. Melting point: 50–51 °C. ^1H NMR (300 MHz, CDCl₃) δ : 3.847 (6H, s, CH₃–O \times 2), 6.959 (2H, d, J = 3.15 Hz, Ar–H), 7.056 (4H, m, Ar–H), 7.208 (2H, d, J = 16 Hz, –COCH=C \times 2), 7.326 (2H, t, J = 8 Hz, Ar–H), 7.699 (2H, d, J = 16 Hz, Ar–CH=C \times 2). ^{13}C NMR (75 MHz, CDCl₃) δ : 55.100, 113.127, 116.158, 120.915, 113.127, 116.158, 120.915, 125.451,

129.759, 135.958, 143.043, 159.751, 188.641. MS (APCI) m/z : 295.0 ($M + 1$) $^+$. HPLC (MeOH:H₂O = 80:20) t_R (min): 6.637. $P_{\text{HPLC}}/\%$: 96.48. HPLC (ACN:H₂O = 80:20) t_R (min): 3.040. $P_{\text{HPLC}}/\%$: 96.71.

4.1.6.13. Compound 2f. IUPAC name: 1,5-bis (4-hydroxy phenyl) penta-1,4-dien-3-one. Dark yellow powder. C₁₇H₁₄O₃. Yield: 24.26%. Melting point: 236–239 °C. ^1H NMR (400 MHz, DMSO- d_6) δ : 10.09 (2H, s), 7.68–7.60 (6H, m), 7.09 (2H, d, J = 16 Hz), 6.83 (4H, d, J = 8.8 Hz). ^{13}C NMR (100 MHz, DMSO- d_6) δ : 115.836, 122.656, 125.821, 130.443, 142.400, 159.821, 188.047. MS (APCI) m/z : 267.2 ($M + 1$) $^+$. HPLC (MeOH:H₂O = 80:20) t_R (min): 2.738. $P_{\text{HPLC}}/\%$: 99.42. HPLC (ACN:H₂O = 70:30) t_R (min): 1.793. $P_{\text{HPLC}}/\%$: 99.67.

4.1.6.14. Compound 2g. IUPAC name: 1,5-bis (3,4-difluoro phenyl) penta-1,4-dien-3-one. Yellow crystals. C₁₇H₁₀F₄O. Yield: 90.0%. Melting point: 132–133 °C. ^1H NMR (300 MHz, DMSO- d_6) δ : 6.955 (2H, d, J = 7.95, Ar–H), 7.199 (2H, t, J = 8.9 Hz, Ar–H), 7.332 (2H, d, J = 16 Hz, –COCH=C \times 2), 7.443 (2H, m, Ar–H), 7.637 (2H, d, J = 16 Hz, Ar–CH=C \times 2). MS (APCI) m/z : 306.9 ($M + 1$) $^+$. HPLC (MeOH:H₂O = 80:20) t_R (min): 2.728. $P_{\text{HPLC}}/\%$: 99.28. HPLC (ACN:H₂O = 70:30) t_R (min): 1.793. $P_{\text{HPLC}}/\%$: 99.67.

4.1.6.15. Compound 3a. IUPAC name: 2,6-bis (4-hydroxy-3-methoxy benzylidene) cyclohexanone. Yellow solid. C₂₂H₂₂O₅. Yield: 30.0%. Melting point: 177–178 °C. ^1H NMR (300 MHz, DMSO, ppm): δ 9.53 (s, 2H), 7.57 (s, 2H), 7.12 (s, 2H), 7.02–7.05 (d, 2H, J = 9 Hz), 6.84–6.87 (d, 2H, J = 9 Hz), 3.82 (s, 6H), 2.90 (s, 4H), 1.71–1.75 (m, 2H); ^{13}C NMR (75 MHz, DMSO, ppm): δ 189.53, 148.87, 148.48, 137.19, 134.55, 127.97, 125.27, 116.59, 115.85, 56.69, 29.01, 23.63. MS (APCI) m/z : 367.0 ($M + 1$) $^+$. HPLC (MeOH:H₂O = 80:20) t_R (min): 3.351. $P_{\text{HPLC}}/\%$: 97.88. HPLC (ACN:H₂O = 80:20) t_R (min): 3.209. $P_{\text{HPLC}}/\%$: 99.31.

4.1.6.16. Compound 3b. IUPAC name: 2,6-bis (3,4-dimethoxy benzylidene) cyclohexanone. Yellow crystals. C₂₄H₂₆O₅. Yield: 47.7%. Melting point: 149–151 °C. ^1H NMR (400 MHz, DMSO, ppm): δ 7.59 (s, 1H), 7.14 (m, 4H), 7.06–6.99 (m, 2H), 3.80 (s, 12H), 2.91 (t, 4H, J = 5.3 Hz), 1.73 (m, 2H); ^{13}C NMR (101 MHz, DMSO, ppm): δ 188.60, 149.47, 148.40, 135.79, 134.26, 128.09, 123.72, 114.01, 111.51, 55.47, 27.82, 22.44. MS (APCI) m/z : 395.1 ($M + 1$) $^+$. HPLC (MeOH:H₂O = 80:20) t_R (min): 5.691. $P_{\text{HPLC}}/\%$: 100.00. HPLC (ACN:H₂O = 80:20) t_R (min): 2.750. $P_{\text{HPLC}}/\%$: 97.80.

4.1.6.17. Compound 3c. IUPAC name: 2,6-bis (3-hydroxy-4-methoxy benzylidene) cyclohexanone. Brownish-yellow powder. C₂₂H₂₂O₅. Yield: 31.09%. Melting point: 189 °C. ^1H NMR (300 MHz, DMSO- d_6 , ppm): δ : 9.18 (br s, 2H), 7.48 (s, 2H), 6.99–7.01 (m, 6H), 3.81 (s, 6H), 2.86 (s, 4H), 1.72 (t, 2H, J = 5 Hz); ^{13}C NMR (75 MHz, DMSO- d_6 , ppm): δ : 188.51, 148.48, 146.17, 135.69, 133.96, 129.17, 122.88, 117.06, 111.91, 55.50, 27.85, 22.24. MS (APCI) m/z : 367.3 ($M + 1$) $^+$. HPLC (MeOH:H₂O = 80:20) t_R (min): 4.810. $P_{\text{HPLC}}/\%$: 100.00. HPLC (ACN:H₂O = 80:20) t_R (min): 1.747. $P_{\text{HPLC}}/\%$: 99.83.

4.1.6.18. Compound 3d. IUPAC name: 2,6-dibenzylidene cyclohexanone. Yellow crystals. C₂₀H₁₈O. Yield: 59.5%. Melting point: 116–120 °C. ^1H NMR (400 MHz, DMSO, ppm): δ 7.63 (s, 2H), 7.53 (d, 4H, J = 7 Hz), 7.46 (dd, 4H, J = 10 Hz), 7.42–7.36 (m, 2H), 2.93–2.84 (m, 4H), 1.75–1.65 (m, 2H); ^{13}C NMR (101 MHz, DMSO, ppm): δ 188.94, 136.25, 135.65, 135.25, 130.23, 128.75, 128.49, 27.76, 22.33. MS (APCI) m/z : 275.1 ($M + 1$) $^+$. HPLC (MeOH:H₂O = 80:20) t_R (min): 12.149. $P_{\text{HPLC}}/\%$: 98.71. HPLC (ACN:H₂O = 80:20) t_R (min): 5.549. $P_{\text{HPLC}}/\%$: 98.60.

4.1.6.19. Compound 3e. IUPAC name: 2,6-bis (3-methoxy benzylidene) cyclohexanone. Yellow crystals. C₂₂H₂₂O₃. Yield: 41.1%.

Melting point: 59–60 °C. ^1H NMR (400 MHz, DMSO, ppm): δ 7.61 (s, 2H), 7.45–7.26 (m, 2H), 7.15–7.00 (m, 4H), 6.99–6.88 (m, 2H), 3.77 (s, 6H), 2.84 (t, 4H, $J = 5.2$ Hz), 1.66 (m, 2H); ^{13}C NMR (101 MHz, DMSO, ppm): δ 188.75, 159.11, 136.59, 136.37, 135.64, 129.43, 122.43, 115.48, 114.45, 54.99, 27.78, 22.28. MS (APCI) m/z : 335.0 ($M + 1$) $^+$. HPLC (MeOH:H₂O = 80:20) t_R (min): 5.049. $P_{\text{HPLC}}/\%$: 95.43. HPLC (ACN:H₂O = 80:20) t_R (min): 4.033. $P_{\text{HPLC}}/\%$: 96.79.

4.1.6.20. Compound 3f. IUPAC name: 2,6-bis (4-hydroxy benzyldene) cyclohexanone. Brownish-yellow powder. C₂₀H₁₈O₃. Yield: 25.44%. Melting point: 270–271 °C. ^1H NMR (400 MHz, DMSO, ppm): δ 7.54 (s, 2H), 7.41 (d, 4H, $J = 8.7$ Hz), 6.88–6.78 (m, 4H), 2.85 (t, 4H, $J = 5.34$ Hz), 1.71 (m, 2H); ^{13}C NMR (101 MHz, DMSO, ppm): δ 188.70, 158.44, 135.92, 133.48, 132.59, 126.59, 115.67, 28.09, 22.67. MS (APCI) m/z : 307.0 ($M + 1$) $^+$. HPLC (MeOH:H₂O = 80:20) t_R (min): 7.542. $P_{\text{HPLC}}/\%$: 98.28. HPLC (ACN:H₂O = 80:20) t_R (min): 3.075. $P_{\text{HPLC}}/\%$: 97.68.

4.1.6.21. Compound 3g. IUPAC name: 2,6-bis (3,4-difluoro benzyldene) cyclohexanone. Yellow crystals. C₂₀H₁₄F₄O. Yield: 12.5%. Melting point: 105–106 °C. ^1H NMR (300 MHz, CDCl₃) δ : 1.79–1.87 (m, 2H, –C–CH₂–), 2.89 (4H, t, $J = 5.7$ Hz, –C–CH₂– $\times 2$), 7.18–7.31 (m, 6H, Ar–H), 7.67 (2H, s, Ar–CH=C $\times 2$). MS (APCI) m/z : 347.0 ($M + 1$) $^+$. HPLC (MeOH:H₂O = 80:20) t_R (min): 6.923. $P_{\text{HPLC}}/\%$: 92.43. HPLC (ACN:H₂O = 80:20) t_R (min): 5.013. $P_{\text{HPLC}}/\%$: 96.79.

4.1.6.22. Compounds 3h. IUPAC name: 2,6-bis (2-fluoro benzyldene) cyclohexanone. Yellow powder. C₂₀H₁₆F₂O. Yield: 98%. Melting point: 95–96 °C. ^1H NMR (300 MHz, CHCl₃) δ : 1.7821 (2H, m, –CH₂–), 2.8086 (4H, t, $J = 5.67$ Hz =C–CH₂– $\times 2$), 7.1324 (4H, m, Ar–H), 7.3441 (4H, m, Ar–H), 7.8224 (2H, s, –CH=C– $\times 2$). ^{13}C NMR (75 MHz, DMSO-*d*₆) δ : 22.9383, 28.5130, 76.5764, 77.0000, 77.4236, 115.5604, 115.8589, 123.6673, 123.7154, 123.7636, 123.9455, 129.7041, 129.7522, 130.2722, 130.3781, 130.6669, 130.7054, 138.1961, 159.1660, 162.4877, 189.5330. MS (APCI) m/z : 311.0 ($M + 1$) $^+$. HPLC (MeOH:H₂O = 80:20) t_R (min): 5.535. $P_{\text{HPLC}}/\%$: 97.00. HPLC (ACN:H₂O = 80:20) t_R (min): 4.435. $P_{\text{HPLC}}/\%$: 95.99.

4.1.6.23. Compound 3i. IUPAC name: 2,6-bis (3-fluoro benzyldene) cyclohexanone. Yellow powder. C₂₀H₁₆F₂O. Yield: 99%. Melting point: 84 °C. ^1H NMR (300 MHz, CHCl₃) δ : 1.8000 (2H, m, –CH₂–), 2.9128 (4H, t, $J = 5.28$ Hz =C–CH₂– $\times 2$), 7.2148 (8H, m, Ar–H $\times 2$), 7.7270 (2H, s, –CH=C– $\times 2$). ^{13}C NMR (75 MHz, DMSO-*d*₆) δ : 22.6206, 28.2241, 76.5764, 77.0000, 77.4236, 115.2909, 115.5701, 116.4452, 116.7351, 126.1321, 126.1706, 129.7619, 129.8678, 135.6254, 135.6542, 135.8577, 137.8206, 137.9265, 160.8509, 164.1148, 189.6774. MS (APCI) m/z : 311.0 ($M + 1$) $^+$. HPLC (MeOH:H₂O = 80:20) t_R (min): 6.683. $P_{\text{HPLC}}/\%$: 99.41. HPLC (ACN:H₂O = 80:20) t_R (min): 5.609. $P_{\text{HPLC}}/\%$: 97.23.

4.1.6.24. Compound 3j. IUPAC name: 2,6-bis (4-fluoro benzyldene) cyclohexanone. Yellow powder. C₂₀H₁₆F₂O. Yield: 99%. Melting point: 151 °C. ^1H NMR (300 MHz, CHCl₃) δ : 1.8055 (2H, m, –CH₂–), 2.8952 (4H, t, $J = 5.28$ Hz =C–CH₂– $\times 2$), 7.0943 (4H, m, Ar–H), 7.4458 (4H, m, Ar–H), 7.7458 (2H, s, –CH=C– $\times 2$). ^{13}C NMR (75 MHz, DMSO-*d*₆) δ : 22.8709, 28.3108, 115.3583, 115.6375, 132.1689, 132.2844, 135.6928, 135.8468, 160.9857, 164.2978, 190.0048. MS (APCI) m/z : 310.9 ($M + 1$) $^+$. HPLC (MeOH:H₂O = 80:20) t_R (min): 5.699. $P_{\text{HPLC}}/\%$: 96.45. HPLC (ACN:H₂O = 80:20) t_R (min): 5.316. $P_{\text{HPLC}}/\%$: 95.44.

4.1.6.25. Compound 4a. IUPAC name: 2,5-bis (4-hydroxy-3-methoxy benzyldene) cyclopentanone. Dark yellow powder. C₂₁H₂₀O₅. Yield: 27.0%. Melting point: 198–202 °C. ^1H NMR (300 MHz, DMSO-*d*₆) δ : 3.06 (4H, s, –CH₂–CH₂–), 3.84 (6H, s,

OCH₃ $\times 2$), 6.89 (2H, d, $J = 8$ Hz, Ar–H), 7.16 (2H, d, $J = 8$ Hz, Ar–H), 7.24 (2H, s, Ar–H), 7.35 (2H, s, CH=C $\times 2$), 9.69 (2H, br s, OH $\times 2$). ^{13}C NMR (75 MHz, DMSO-*d*₆) δ : 26.914, 56.605, 115.545, 116.922, 125.793, 128.179, 133.841, 135.768, 148.727, 149.537, 195.480. MS (APCI) m/z : 353.0 ($M + 1$) $^+$. HPLC (MeOH:H₂O = 80:20) t_R (min): 2.464. $P_{\text{HPLC}}/\%$: 98.66. HPLC (ACN:H₂O = 70:30) t_R (min): 1.953. $P_{\text{HPLC}}/\%$: 100.00.

4.1.6.26. Compound 4b. IUPAC name: 2,5-bis (3,4-dimethoxy benzyldene) cyclopentanone. Yellow powder. C₂₃H₂₄O₅. Yield: 44.0%. Melting point: 196–199 °C. ^1H NMR (300 MHz, CDCl₃) δ : 3.10 (4H, s, CH₂–CH₂–), 3.93 (12H, s, OCH₃ $\times 4$), 6.93 (2H, d, $J = 8$ Hz, Ar–H), 7.12–7.27 (m, 4H, Ar–H), 7.53 (2H, s, CH=C $\times 2$). ^{13}C NMR (75 MHz, DMSO-*d*₆) δ : 26.387, 55.822, 55.899, 111.112, 113.409, 124.534, 128.946, 133.622, 135.319, 148.856, 150.223, 195.946. MS (APCI) m/z : 381.0 ($M + 1$) $^+$. HPLC (MeOH:H₂O = 80:20) t_R (min): 7.734. $P_{\text{HPLC}}/\%$: 96.91. HPLC (ACN:H₂O = 80:20) t_R (min): 2.377. $P_{\text{HPLC}}/\%$: 96.60.

4.1.6.27. Compound 4c. IUPAC name: 2,5-bis (3-hydroxy-4-methoxy benzyldene) cyclopentanone. Dark yellow powder. C₂₁H₂₀O₅. Yield: 27.19%. Melting point: 224–225 °C. ^1H NMR (300 MHz, DMSO-*d*₆) δ : 3.02 (4H, s, CH₂–CH₂–), 3.82 (6H, s, OCH₃ $\times 2$), 7.02 (2H, d, $J = 8$ Hz, Ar–H), 7.12–7.14 (m, 4H, Ar–H), 7.28 (2H, s, CH=C $\times 2$), 9.28 (2H, s, OH $\times 2$). ^{13}C NMR (75 MHz, DMSO-*d*₆) δ : 25.846, 55.534, 112.095, 116.836, 123.566, 128.334, 132.410, 135.260, 146.481, 149.148, 194.795. MS (APCI) m/z : 353.0 ($M + 1$) $^+$. HPLC (MeOH:H₂O = 80:20) t_R (min): 6.566. $P_{\text{HPLC}}/\%$: 99.28. HPLC (ACN:H₂O = 80:20) t_R (min): 3.083. $P_{\text{HPLC}}/\%$: 99.79.

4.1.6.28. Compound 4d. IUPAC name: 2,5-dibenzylidene cyclopentanone. Yellow powder. C₁₉H₁₆O. Yield: 63.9%. Melting point: 194–195 °C. ^1H NMR (400 MHz, CDCl₃) δ : 7.61–7.59 (6H, m), 7.46–7.36 (6H, m), 3.11 (4H, s). ^{13}C NMR (100 MHz, CDCl₃) δ : 26.434, 128.675, 129.286, 130.652, 133.722, 135.717, 137.212, 196.220. MS (APCI) m/z : 381.0 ($M + 1$) $^+$. HPLC (MeOH:H₂O = 80:20) t_R (min): 22.011. $P_{\text{HPLC}}/\%$: 97.12. HPLC (ACN:H₂O = 80:20) t_R (min): 4.199. $P_{\text{HPLC}}/\%$: 99.28.

4.1.6.29. Compound 4e. IUPAC name: 2,5-bis (3-methoxy benzyldene) cyclopentanone. Yellow crystals. C₂₁H₂₀O₃. Yield: 56.8%. Melting point: 144–147 °C. ^1H NMR (300 MHz, CDCl₃) δ : 3.05 (4H, s, CH₂–CH₂–), 3.82 (6H, s, MeO $\times 2$), 6.91 (dd, $J = 2$ Hz, $J = 10$ Hz, 2H, Ar–H), 7.08 (s, 2H, Ar–H), 7.16 (d, $J = 8$ Hz, 2H, Ar–H), 7.30–7.35 (m, 2H, Ar–H), 7.52 (s, 2H, CH=C $\times 2$). ^{13}C NMR (75 MHz, DMSO-*d*₆) δ : 26.387, 55.154, 114.968, 115.888, 123.179, 129.592, 133.647, 136.978, 137.405, 159.579, 196.103. MS (APCI) m/z : 321.0 ($M + 1$) $^+$. HPLC (MeOH:H₂O = 80:20) t_R (min): 13.048. $P_{\text{HPLC}}/\%$: 98.85. HPLC (ACN:H₂O = 80:20) t_R (min): 4.022. $P_{\text{HPLC}}/\%$: 99.09.

4.1.6.30. Compound 4f. IUPAC name: 2,5-bis (4-hydroxy benzyldene) cyclopentanone. Greenish-yellow powder. C₁₉H₁₆O₃. Yield: 31.60%. Melting point: 314 °C. ^1H NMR (300 MHz, DMSO-*d*₆) δ : 3.02 (4H, s, CH₂–CH₂–), 6.87 (4H, d, $J = 8$ Hz, Ar–H^{3.5} $\times 2$), 7.33 (s, 2H, CH=C $\times 2$), 7.54 (4H, d, $J = 8$ Hz, Ar–H^{2.6} $\times 2$), 10.1 (br s, 2H, OH $\times 2$). ^{13}C NMR (75 MHz, DMSO-*d*₆) δ : 26.063, 116.110, 126.800, 132.912, 134.787, 159.078, 195.280. MS (APCI) m/z : 293.0 ($M + 1$) $^+$. HPLC (MeOH:H₂O = 80:20) t_R (min): 3.854. $P_{\text{HPLC}}/\%$: 98.60. HPLC (ACN:H₂O = 70:30) t_R (min): 1.784. $P_{\text{HPLC}}/\%$: 99.66.

4.1.6.31. Compound 4g. IUPAC name: 2,5-bis (3,4-difluoro benzyldene) cyclopentanone. Yellow crystals. C₁₉H₁₂F₄O. Yield: 38.5%. Melting point: 239–240 °C. ^1H NMR (300 MHz, CDCl₃) δ : 3.10 (4H, s, CH₂–CH₂–), 7.19–7.45 (m, 6H, Ar–H), 7.50 (s, 2H, CH=C $\times 2$). MS (APCI) m/z : 332.9 ($M + 1$) $^+$. HPLC (MeOH:H₂O = 80:20) t_R (min):

20.240. $P_{\text{HPLC}}/\%$: 96.92. HPLC (ACN:H₂O = 70:30) t_{R} (min): 13.712. $P_{\text{HPLC}}/\%$: 98.41.

4.1.6.32. **Compound 4h**. IUPAC name: 2,5-bis (2-fluoro benzyli-dene) cyclopentanone. Yellow powder. C₁₉H₁₄F₂O. Yield: 99%. Melting point: 210 °C. ¹H NMR (300 MHz, CHCl₃) δ : 3.0484 (4H, s, CH₂–CH₂), 7.7167 (4H, m, Ar–H), 7.3667 (2H, m, Ar–H), 7.5776 (2H, m, Ar–H), 7.8111 (2H, s, Ar–CH=C \times 2). ¹³C NMR (75 MHz, DMSO-*d*₆) δ : 26.0771, 76.1527, 76.5764, 77.0000, 115.3775, 115.6664, 123.3496, 123.5132, 123.6095, 123.6577, 125.2655, 125.3329, 129.7041, 130.5802, 130.6958, 138.5041, 159.6281, 195.1076. MS (APCI) m/z : 297.0 (M + 1)⁺. HPLC (MeOH:H₂O = 80:20) t_{R} (min): 6.816. $P_{\text{HPLC}}/\%$: 99.89. HPLC (ACN:H₂O:80 = 20) t_{R} (min): 4.057. $P_{\text{HPLC}}/\%$: 94.18.

4.1.6.33. **Compound 4i**. IUPAC name: 2,5-bis (3-fluoro benzyli-dene) cyclopentanone. Yellow powder. C₁₉H₁₄F₂O. Yield: 99%. Melting point: 191–192 °C. ¹H NMR (300 MHz, CHCl₃) δ : 2.9969 (4H, s, CH₂–CH₂), 7.0071 (2H, m, Ar–H), 7.2633 (6H, m, Ar–H), 7.4257 (2H, s, Ar–CH=C \times 2). ¹³C NMR (75 MHz, DMSO-*d*₆) δ : 26.3370, 76.5764, 77.0000, 77.4236, 100.6658, 116.1863, 116.4751, 116.5907, 116.8795, 126.7001, 126.7386, 130.1662, 130.2818, 132.7273, 132.7658, 137.6954, 137.8109, 138.0420, 139.6595, 161.1494, 164.4229, 195.9068. MS (APCI) m/z : 297.0 (M + 1)⁺. HPLC (MeOH:H₂O = 80:20) t_{R} (min): 5.848. $P_{\text{HPLC}}/\%$: 97.32. HPLC (ACN:H₂O = 80:20) t_{R} (min): 4.303. $P_{\text{HPLC}}/\%$: 93.77.

4.1.6.34. **Compound 4j**. IUPAC name: 2,5-bis (4-fluoro benzyli-dene) cyclopentanone. Yellow powder. C₁₉H₁₄F₂O. Yield: 99%. Melting point: 239–240 °C. ¹H NMR (300 MHz, CHCl₃) δ : 2.7885 (4H, s, CH₂–CH₂), 6.8292 (8H, m, Ar–H), 7.3077 (2H, s, Ar–CH=C \times 2). ¹³C NMR (75 MHz, DMSO-*d*₆) δ : 26.3274, 76.5764, 77.0000, 77.4236, 115.8108, 116.0996, 131.9956, 132.0437, 132.5444, 132.6599, 132.7177, 136.6556, 161.4864, 164.8177, 196.0416. MS (APCI) m/z : 297.0 (M + 1)⁺. HPLC (MeOH:H₂O = 80:20) t_{R} (min): 7.108. $P_{\text{HPLC}}/\%$: 99.57. HPLC (ACN:H₂O = 80:20) t_{R} (min): 4.387. $P_{\text{HPLC}}/\%$: 95.02.

4.1.6.35. **Compound 5a**. IUPAC name: 1,3-bis (4-hydroxy-3-methoxy phenyl) prop-2-en-1-one. Yellow powder. C₁₇H₁₆O₅. Yield: 34.07%. Melting point: 108–110 °C. ¹H NMR (400 MHz, DMSO-*d*₆) δ : 10.01 (1H, s), 9.68 (1H, s), 7.79–7.71 (2H, m), 7.63–7.59 (2H, m), 7.47 (1H, d, J = 1.6 Hz), 7.28–7.25 (1H, m), 6.91 (1H, d, J = 8.4 Hz), 6.83 (1H, d, J = 8.4 Hz), 3.86 (6H, s). ¹³C NMR (100 MHz, DMSO-*d*₆) δ : 55.637, 55.776, 111.519, 111.722, 114.848, 115.540, 118.643, 123.480, 126.445, 129.786, 143.527, 147.711, 149.334, 151.593, 186.957. MS (APCI) m/z : 301.0 (M + 1)⁺. HPLC (MeOH:H₂O = 80:20) t_{R} (min): 4.252. $P_{\text{HPLC}}/\%$: 97.30. HPLC (ACN:H₂O = 80:20) t_{R} (min): 3.234. $P_{\text{HPLC}}/\%$: 95.49.

4.1.6.36. **Compound 5b**. IUPAC name: 1,3-bis (3,4-dimethoxy phenyl) prop-2-en-1-one. Light yellow solid. C₁₉H₂₀O₅. Yield: 69.0%. Melting point: 110 °C. ¹H NMR (400 MHz, CDCl₃) δ : 7.92–7.89 (1H, m), 7.81 (1H, d, J = 15.6 Hz), 7.67 (1H, d, J = 15.2 Hz), 7.59 (1H, d, J = 1.6 Hz), 7.51 (1H, d, J = 1.6 Hz), 7.40–7.37 (1H, m), 7.09 (1H, d, J = 8.4 Hz), 7.01 (1H, d, J = 18.4 Hz), 3.86–3.85 (9H, m), 3.81 (3H, s). ¹³C NMR (100 MHz, CDCl₃) δ : 187.35, 153.06, 151.09, 148.98, 148.78, 143.53, 130.75, 127.63, 123.50, 123.25, 119.57, 111.57, 110.99, 110.78, 110.73, 55.72, 55.56. MS (APCI) m/z : 329.0 (M + 1)⁺. HPLC (MeOH:H₂O = 80:20) t_{R} (min): 7.043. $P_{\text{HPLC}}/\%$: 99.34. HPLC (ACN:H₂O = 80:20) t_{R} (min): 3.742. $P_{\text{HPLC}}/\%$: 99.12.

4.1.6.37. **Compound 5c**. IUPAC name: 1,3-bis (3-hydroxy-4-methoxy phenyl) prop-2-en-1-one. Yellow powder. C₁₇H₁₆O₅. Yield: 34.1%. Melting point: 144–147 °C. ¹H NMR (300 MHz, CDCl₃)

δ : 3.94 (s, 3H, OCH₃), 3.98 (s, 3H, OCH₃), 6.86 (d, J = 8 Hz, 1H, Ar–H), 6.93 (d, J = 8 Hz, 1H, Ar–H), 7.13 (dd, J = 1.8 Hz, J = 10 Hz, 1H, Ar–H), 7.27–7.28 (m, 1H, Ar–H), 7.39 (d, J = 16 Hz, 1H, COCH=), 7.61–7.63 (m, 2H, Ar–H), 7.72 (d, J = 16 Hz, 1H, ArCH=). ¹³C NMR (75 MHz, DMSO-*d*₆) δ : 56.197, 56.288, 111.821, 112.542, 114.804, 115.151, 119.781, 122.406, 122.779, 128.088, 131.317, 144.265, 146.882, 147.027, 150.793, 152.766, 188.593. MS (APCI) m/z : 301.0 (M + 1)⁺. HPLC (MeOH:H₂O = 80:20) t_{R} (min): 3.366. $P_{\text{HPLC}}/\%$: 99.40. HPLC (ACN:H₂O = 80:20) t_{R} (min): 2.934. $P_{\text{HPLC}}/\%$: 99.91.

4.1.6.38. **Compound 5d**. IUPAC name: 1,3-diphenyl prop-2-en-1-one. Light yellow crystals. C₁₅H₁₂O. Yield: 66.1%. Melting point: 53–55 °C. ¹H NMR (400 MHz, CDCl₃) δ : 8.04–8.02 (2H, m), 7.82 (1H, d, J = 15.6 Hz), 7.66–7.64 (2H, m), 7.61–7.49 (4H, m), 7.43–7.41 (3H, m). ¹³C NMR (100 MHz, CDCl₃) δ : 190.51, 144.79, 138.20, 134.88, 132.73, 130.49, 128.92, 128.58, 128.47, 128.41, 122.11. MS (APCI) m/z : 209.0 (M + 1)⁺. HPLC (MeOH:H₂O = 80:20) t_{R} (min): 8.273. $P_{\text{HPLC}}/\%$: 100.00. HPLC (ACN:H₂O = 70:30) t_{R} (min): 4.465. $P_{\text{HPLC}}/\%$: 99.27.

4.1.6.39. **Compound 5e**. IUPAC name: 1,3-bis (3-methoxy phenyl) prop-2-en-1-one. Yellow liquid. C₁₇H₁₆O₃. Yield: 15.8%. Liquid state. ¹H NMR (300 MHz, CDCl₃) δ : 3.85 (s, 3H, OMe), 3.88 (s, 3H, OMe), 6.97 (d, J = 8 Hz, 1H, Ar–H), 7.12–7.61 (m, 8H, Ar–H + COCH=), 7.77 (d, J = 16 Hz, 1H, Ar–CH=). ¹³C NMR (75 MHz, CDCl₃) δ : 121.980, 128.358, 55.038, 55.156, 112.704, 113.263, 116.053, 118.978, 120.818, 120.857, 122.060, 129.343, 129.696, 135.993, 144.437, 159.650, 159.700, 189.78. MS (APCI) m/z : 241.2 (M + 1)⁺. HPLC (MeOH:H₂O = 80:20) t_{R} (min): 6.073. $P_{\text{HPLC}}/\%$: 98.13. HPLC (ACN:H₂O = 70:30) t_{R} (min): 2.867. $P_{\text{HPLC}}/\%$: 97.85.

4.1.6.40. **Compound 5f**. IUPAC name: 1,3-bis (4-hydroxy phenyl) prop-2-en-1-one. Pale yellow powder. C₁₅H₁₂O₃. Yield: 12.05%. Melting point: 190–195 °C. ¹H NMR (300 MHz, DMSO-*d*₆) δ : 6.80–6.88 (m, 4H, Ar–H), 7.56–7.62 (m, 4H, Ar–H + –CH=CH–), 7.94 (d, J = 8 Hz, 2H, Ar–H). MS (APCI) m/z : 241.2 (M + 1)⁺. HPLC (MeOH:H₂O = 80:20) t_{R} (min): 3.326. $P_{\text{HPLC}}/\%$: 99.69. HPLC (ACN:H₂O = 70:30) t_{R} (min): 2.941. $P_{\text{HPLC}}/\%$: 99.69.

4.1.6.41. **Compound 5g**. IUPAC name: 1,3-bis (3,4-difluoro phenyl) prop-2-en-1-one. White crystals. C₁₅H₈F₄O. Yield: 14.3%. Melting point: 132–134 °C. ¹H NMR (300 MHz, CDCl₃) δ : 7.18–7.39 (m, 4H, Ar–H + COCH=), 7.45–7.51 (m, 1H, Ar–H), 7.73 (d, J = 16 Hz, 1H, Ar–CH=), 7.79–7.90 (m, 2H, Ar–H). ¹³C NMR (75 MHz, CDCl₃) δ : 55100.711, 116.482, 116.715, 117.508, 117.742, 117.894, 117.978, 118.127, 121.670, 121.694, 125.335, 125.403, 131.783, 131.841, 134.884, 143.229, 148.946, 152.249, 187.095. MS (APCI) m/z : 280.9 (M + 1)⁺. HPLC (MeOH:H₂O = 80:20) t_{R} (min): 4.523. $P_{\text{HPLC}}/\%$: 95.64. HPLC (ACN:H₂O = 80:20) t_{R} (min): 3.812. $P_{\text{HPLC}}/\%$: 96.05.

4.2. Biology

4.2.1. Cell lines and plasmids

All cell culture reagents were procured from Sigma Chemical Co. (St Louis, MO). The U2OS human osteosarcoma cell line was bought from American Tissue Culture Collection (Rockville, MD) and grown and maintained in McCoy's 5A medium. The human embryonic kidney cells (HEK293T) was a gift from Dr Yi Yan Yang (Institute of Biotechnology and Nanotechnology, Singapore). These cells were cultured and maintained in Dulbecco's Modified Eagle's Medium (DMEM). Both L-cells and L-cells stably transfected with a Wnt-3A expression factor (L-Wnt-3A cells) were kindly provided by Professor Victor Nurcombe (Institute of Medical Biology, A*STAR, Singapore) and were maintained in DMEM supplemented with 400 μ g/mL of G418. All culture media were supplemented with 10%

fetal bovine serum (FBS) (Invitrogen, Carlsbad, CA), 100 µg/mL streptomycin and 10 U/mL of penicillin G. The cells were grown in a humidified atmosphere at 37 °C containing 5% CO₂. Wnt-3A conditioned medium (Wnt-3A CM) was prepared from Wnt-3A secreting L-Wnt-3A cells according to ATCC instructions. TOPglow and FOPglow reporter genes were purchased from Upstate Biotechnology (Lake Placid, NY). The pCMV-RL renilla control vector was purchased from Promega (Madison, WI). The synthesized curcumin analogs were dissolved in dimethyl sulfoxide (DMSO) with the absolute concentration of DMSO not exceeding 0.1% in all the experiments.

4.2.2. Dual luciferase reporter assay

HEK293T cells (1.4×10^6) grown to 40% confluency in 60 mm culture dish were transiently co-transfected with either 3 µg TOPglow or 3 µg FOPglow and 0.012 µg pCMV-RL renilla control plasmids for normalization of transfection efficiency using Lipofectamine 2000 (Invitrogen, Carlsbad, CA), following manufacturer's instructions. On the other hand, U2OS cells (1.0×10^5 /well) were grown in 24-well plates to 90–95% confluency and then transiently co-transfected with either 0.3 µg TOPglow or 0.3 µg FOPglow, and 0.012 µg pCMV-RL renilla plasmids. Twenty hours post transfection, both the cell types were co-incubated with Wnt-3A CM and curcumin analogs at various concentrations (0.01–20 µM) for 24 h. For HEK293T cells, they were re-seeded into 96-well plates at a density of 18×10^3 cells/well before treatment. Luciferase assays were performed with the Dual Luciferase Reporter assay system (Promega, Madison, WI) as per manufacturer's instructions. Briefly, 20 µL cell lysate was incubated with 100 µL Dual-Glo[®] Luciferase Reagent followed by incubation with 100 µL of Dual-Glo[®] Stop & Glo[®] Reagent and the luminescence was measured at both the steps with a luminometer (Tecan, MTX Lab Systems Inc., Vienna, VA). All the readings were performed in triplicates and expressed as mean \pm S.E.M. of the normalized ratios of Firefly to Renilla luciferase and as the percentage of DMSO-treated samples. The EC₅₀ values for HEK293T cells were obtained from the sigmoidal curve by plotting the percentage normalized luciferase activity against the concentration of curcumin analogs using GraphPad Prism version 4.00, GraphPad Software (San Diego, CA).

4.2.3. MTS assay

MTS cell cytotoxicity assay was used to evaluate the cytotoxic profile of the curcumin analogs. HEK293T and U2OS cells were seeded into 96-well plates at a density of 18×10^3 cells/well and 10×10^3 cells/well, respectively. On the subsequent day, HEK293T cells were treated with curcumin analogs at their respective EC₅₀ concentrations for Wnt inhibition for 24 h while U2OS cells were treated with curcumin analogs at 1 and 5 µM for 24 h. After treatment, cell viability was analyzed by adding 20 µL of CellTiter 96 AQueous One Solution Reagent (Promega, Madison, WI). Following an incubation period of 4 h, the absorbance of the formed formazan crystals was measured at λ_{max} of 490 nm using a Tecan Spectra Fluor spectrophotometer (MTX Lab Systems Inc Vienna, VA). The percent cell viability after treatment with curcumin analogs was calculated using the following formula: % viability = $(A_{\text{Analogues}} - A_{\text{Blank}}) / (A_{\text{Control (DMSO)}} - A_{\text{Blank}}) \times 100\%$, where $A_{\text{Analogues}}$ = absorbance of wells with cells treated with curcumin analogs, A_{Blank} = absorbance of wells with media and $A_{\text{Control (DMSO)}}$ = absorbance of wells with DMSO treated cells. Each concentration of curcumin analog was performed in triplicate on three separate occasions.

4.2.4. Cell invasion assay

Matrigel invasion assay was used to determine the effect of curcumin analogs on U2OS cell invasion as previously described [12].

We used 30 µg Matrigel (BD Bioscience, San Jose, CA) precoated 8 µm pore size polyethylene terephthalate (PET) membrane inserts (BD Bioscience, San Jose, CA) for the assay. U2OS cells were treated with different concentrations of curcumin analogs for 24 h. The viability of the cells was confirmed by trypan blue exclusion assay before they were seeded onto the upper wells of the precoated membrane inserts at a density of 1.5×10^5 /200 µL in serum-free medium. McCoy's 5A medium with 15% FBS was added as a chemoattractant in the lower compartment while control wells contained serum-free medium in the lower chamber. Pre-treated U2OS cells were allowed to invade the matrigel coated inserts for 48 h, following which the non-invasive cells were removed with the help of a cotton swab. Cells in the lower surface of the membrane were then fixed with 70% ethanol and stained with 0.2% w/v crystal violet. Ten random microscopic fields (200 \times magnifications) were counted for invaded cells using Nikon Eclipse TE2000U microscope (Melville, NY). All experiments were performed at least in triplicates.

4.2.5. Western blot analysis

The expression levels of β -catenin and MMP-9 protein was examined pre- and post-24 h treatment with curcumin analogs using western blot analysis as previously described [12]. β -Catenin and MMP-9 primary antibodies were obtained from Santa Cruz Biotechnology, Inc. (Santa Cruz, CA), whereas those for lamin A/C and α -tubulin were purchased from Sigma Chemical Co. (St Louis, MO) and BD Bioscience (San Jose, CA), respectively. Anti-mouse IgG horseradish peroxidase secondary antibody was from Bio-Rad (Hercules, CA). Quantity One software (Bio-Rad, Hercules, CA) was used for quantifying the bands and the results were then expressed relative to the lamin A/C and α -tubulin loading controls. All western blot experiments were repeated at least in triplicates.

4.2.5.1. Statistical analysis. The two-tailed Student's *t*-test (SPSS, Chicago, IL) was used to analyze statistical significance for treatment groups. *p*-value of less than 0.05 was used for statistical comparison between the treated and the control samples.

Acknowledgments

We thank Dr Yi-Yan Yang and Professor Victor Nurcombe for providing the HEK293T cells and L Wnt-3A cells respectively. We also thank A/Prof Mei Lin Go for her helpful comments and suggestions. This work was made possible by the Ministry of Education Academic Research Fund (AcRF) R148000150112 to PLRE and National University of Singapore Graduate Scholarships to PCL, KLT and PB.

Appendix A. Supplementary data

Supplementary data related to this article can be found at <http://dx.doi.org/10.1016/j.ejmech.2013.10.073>.

References

- [1] C.A. Arndt, W.M. Crist, Common musculoskeletal tumors of childhood and adolescence, *N. Engl. J. Med.* 341 (1999) 342–352.
- [2] P.A. Meyers, G. Heller, J.H. Healey, A. Huvos, A. Applewhite, M. Sun, M. LaQuaglia, Osteogenic sarcoma with clinically detectable metastasis at initial presentation, *J. Clin. Oncol.* 11 (1993) 449–453.
- [3] H.C. Crawford, B.M. Fingleton, L.A. Rudolph-Owen, K.J. Goss, B. Rubinfeld, P. Polakis, L.M. Matrisian, The metalloproteinase matrilysin is a target of beta-catenin transactivation in intestinal tumors, *Oncogene* 18 (1999) 2883–2891.
- [4] T.C. He, A.B. Sparks, C. Rago, H. Hermeking, L. Zawal, L.T. da Costa, P.J. Morin, B. Vogelstein, K.W. Kinzler, Identification of c-MYC as a target of the APC pathway, *Science* 281 (1998) 1509–1512.
- [5] O. Tetsu, F. McCormick, Beta-catenin regulates expression of cyclin D1 in colon carcinoma cells, *Nature* 398 (1999) 422–426.

- [6] R.C. Haydon, A. Deyrup, A. Ishikawa, R. Heck, W. Jiang, L. Zhou, T. Feng, D. King, H. Cheng, B. Breyer, T. Peabody, M.A. Simon, A.G. Montag, T.C. He, Cytoplasmic and/or nuclear accumulation of the beta-catenin protein is a frequent event in human osteosarcoma, *Int. J. Cancer* 102 (2002) 338–342.
- [7] K. Iwao, Y. Miyoshi, G. Nawa, H. Yoshikawa, T. Ochi, Y. Nakamura, Frequent beta-catenin abnormalities in bone and soft-tissue tumors, *Jpn. J. Cancer Res.* 90 (1999) 205–209.
- [8] K. Chen, S. Fallen, H.O. Abaan, M. Hayran, C. Gonzalez, F. Wodajo, T. MacDonald, J.A. Toretsky, A. Uren, Wnt10b induces chemotaxis of osteosarcoma and correlates with reduced survival, *Pediatr. Blood Cancer* 51 (2008) 349–355.
- [9] B.H. Hoang, T. Kubo, J.H. Healey, R. Sowers, B. Mazza, R. Yang, A.G. Huvo, P.A. Meyers, R. Gorlick, Expression of LDL receptor-related protein 5 (LRP5) as a novel marker for disease progression in high-grade osteosarcoma, *Int. J. Cancer* 109 (2004) 106–111.
- [10] Y. Guo, X. Zi, Z. Koontz, A. Kim, J. Xie, R. Gorlick, R.F. Holcombe, B.H. Hoang, Blocking Wnt/LRP5 signaling by a soluble receptor modulates the epithelial to mesenchymal transition and suppresses met and metalloproteinases in osteosarcoma Saos-2 cells, *J. Orthop. Res.* 25 (2007) 964–971.
- [11] Y. Guo, E.M. Rubin, J. Xie, X. Zi, B.H. Hoang, Dominant negative LRP5 decreases tumorigenicity and metastasis of osteosarcoma in an animal model, *Clin. Orthop. Relat. Res.* 466 (2008) 2039–2045.
- [12] P.C. Leow, Q. Tian, Z.Y. Ong, Z. Yang, P.L. Ee, Antitumor activity of natural compounds, curcumin and PKF118-310, as Wnt/beta-catenin antagonists against human osteosarcoma cells, *Invest New Drugs* 28 (2010) 766–782.
- [13] D.J. Newman, G.M. Cragg, Natural products as sources of new drugs over the last 25 years, *J. Nat. Prod.* 70 (2007) 461–477.
- [14] Y.J. Surh, Cancer chemoprevention with dietary phytochemicals, *Nat. Rev. Cancer* 3 (2003) 768–780.
- [15] C. Sharma, J. Kaur, S. Shishodia, B.B. Aggarwal, R. Ralhan, Curcumin down regulates smokeless tobacco-induced NF-kappaB activation and COX-2 expression in human oral premalignant and cancer cells, *Toxicology* 228 (2006) 1–15.
- [16] S. Singh, B.B. Aggarwal, Activation of transcription factor NF-kappa B is suppressed by curcumin (diferuloylmethane) [corrected], *J. Biol. Chem.* 270 (1995) 24995–25000.
- [17] A.P. Zambre, V.M. Kulkarni, S. Padhye, S.K. Sandur, B.B. Aggarwal, Novel curcumin analogs targeting TNF-induced NF-kappaB activation and proliferation in human leukemic KBM-5 cells, *Bioorg. Med. Chem.* 14 (2006) 7196–7204.
- [18] N. Dhillon, B.B. Aggarwal, R.A. Newman, R.A. Wolff, A.B. Kunnumakkara, J.L. Abbruzzese, C.S. Ng, V. Badmaev, R. Kurzrock, Phase II trial of curcumin in patients with advanced pancreatic cancer, *Clin. Cancer Res.* 14 (2008) 4491–4499.
- [19] S. Balasubramanian, R.L. Eckert, Curcumin suppresses AP1 transcription factor-dependent differentiation and activates apoptosis in human epidermal keratinocytes, *J. Biol. Chem.* 282 (2007) 6707–6715.
- [20] Y.J. Surh, S.S. Han, Y.S. Keum, H.J. Seo, S.S. Lee, Inhibitory effects of curcumin and capsaicin on phorbol ester-induced activation of eukaryotic transcription factors, NF-kappaB and AP-1, *BioFactors* 12 (2000) 107–112.
- [21] A.C. Bharti, N. Donato, B.B. Aggarwal, Curcumin (diferuloylmethane) inhibits constitutive and IL-6-inducible STAT3 phosphorylation in human multiple myeloma cells, *J. Immunol.* 171 (2003) 3863–3871.
- [22] S. Bhattacharyya, D. Mandal, B. Saha, G.S. Sen, T. Das, G. Sa, Curcumin prevents tumor-induced T cell apoptosis through Stat-5a-mediated Bcl-2 induction, *J. Biol. Chem.* 282 (2007) 15954–15964.
- [23] R. Blasius, S. Reuter, E. Henry, M. Dicato, M. Diederich, Curcumin regulates signal transducer and activator of transcription (STAT) expression in K562 cells, *Biochem. Pharmacol.* 72 (2006) 1547–1554.
- [24] H.Y. Kim, E.J. Park, E.H. Joe, I. Jou, Curcumin suppresses Janus kinase-STAT inflammatory signaling through activation of Src homology 2 domain-containing tyrosine phosphatase 2 in brain microglia, *J. Immunol.* 171 (2003) 6072–6079.
- [25] C. Natarajan, J.J. Bright, Curcumin inhibits experimental allergic encephalomyelitis by blocking IL-12 signaling through Janus kinase-STAT pathway in T lymphocytes, *J. Immunol.* 168 (2002) 6506–6513.
- [26] J. Rajasingh, H.P. Raikwar, G. Muthian, C. Johnson, J.J. Bright, Curcumin induces growth-arrest and apoptosis in association with the inhibition of constitutively active JAK-STAT pathway in T cell leukemia, *Biochem. Biophys. Res. Commun.* 340 (2006) 359–368.
- [27] M. Saydmohammed, D. Joseph, V. Syed, Curcumin suppresses constitutive activation of STAT-3 by up-regulating protein inhibitor of activated STAT-3 (PIAS-3) in ovarian and endometrial cancer cells, *J. Cell Biochem.* 110 (2010) 447–456.
- [28] Y. Chen, W. Shu, W. Chen, Q. Wu, H. Liu, G. Cui, Curcumin, both histone deacetylase and p300/CBP-specific inhibitor, represses the activity of nuclear factor kappa B and Notch 1 in Raji cells, *Basic Clin. Pharmacol. Toxicol.* 101 (2007) 427–433.
- [29] Z. Wang, Y. Zhang, S. Banerjee, Y. Li, F.H. Sarkar, Notch-1 down-regulation by curcumin is associated with the inhibition of cell growth and the induction of apoptosis in pancreatic cancer cells, *Cancer* 106 (2006) 2503–2513.
- [30] A.S. Jaiswal, B.P. Marlow, N. Gupta, S. Narayan, Beta-catenin-mediated trans-activation and cell-cell adhesion pathways are important in curcumin (diferuloylmethane)-induced growth arrest and apoptosis in colon cancer cells, *Oncogene* 21 (2002) 8414–8427.
- [31] M. Kakarala, D.E. Brenner, H. Korkaya, C. Cheng, K. Tazi, C. Ginestier, S. Liu, G. Dontu, M.S. Wicha, Targeting breast stem cells with the cancer preventive compounds curcumin and piperine, *Breast Cancer Res. Treat.* 122 (2010) 777–785.
- [32] C.H. Park, E.R. Hahm, S. Park, H.K. Kim, C.H. Yang, The inhibitory mechanism of curcumin and its derivative against beta-catenin/Tcf signaling, *FEBS Lett.* 579 (2005) 2965–2971.
- [33] G. Garcea, D.P. Berry, D.J. Jones, R. Singh, A.R. Dennison, P.B. Farmer, R.A. Sharma, W.P. Steward, A.J. Gescher, Consumption of the putative chemopreventive agent curcumin by cancer patients: assessment of curcumin levels in the colorectum and their pharmacodynamic consequences, *Cancer Epidemiol. Biomarkers Prev.* 14 (2005) 120–125.
- [34] R.A. Sharma, S.A. Euden, S.L. Platten, D.N. Cooke, A. Shafayat, H.R. Hewitt, T.H. Marczylo, B. Morgan, D. Hemingway, S.M. Plummer, M. Pirmohamed, A.J. Gescher, W.P. Steward, Phase I clinical trial of oral curcumin: biomarkers of systemic activity and compliance, *Clin. Cancer Res.* 10 (2004) 6847–6854.
- [35] A.L. Cheng, C.H. Hsu, J.K. Lin, M.M. Hsu, Y.F. Ho, T.S. Shen, J.Y. Ko, J.T. Lin, B.R. Lin, W. Ming-Shiang, H.S. Yu, S.H. Jee, G.S. Chen, T.M. Chen, C.A. Chen, M.K. Lai, Y.S. Pu, M.H. Pan, Y.J. Wang, C.C. Tsai, C.Y. Hsieh, Phase I clinical trial of curcumin, a chemopreventive agent, in patients with high-risk or pre-malignant lesions, *Anticancer Res.* 21 (2001) 2895–2900.
- [36] M.M. Yallapu, M. Jaggi, S.C. Chauhan, Curcumin nanoformulations: a future nanomedicine for cancer, *Drug Discov. Today* 17 (2012) 71–80.
- [37] A. Vyas, P. Dandawate, S. Padhye, A. Ahmad, F. Sarkar, Perspectives on new synthetic curcumin analogs and their potential anticancer properties, *Curr. Pharm. Des.* 19 (2013) 2047–2069.
- [38] C. Zhao, Z. Liu, G. Liang, Promising curcumin-based drug design: mono-carbonyl analogues of curcumin (MACs), *Curr. Pharm. Des.* 19 (2013) 2114–2135.
- [39] G. Liang, L. Shao, Y. Wang, C. Zhao, Y. Chu, J. Xiao, Y. Zhao, X. Li, S. Yang, Exploration and synthesis of curcumin analogues with improved structural stability both in vitro and in vivo as cytotoxic agents, *Bioorg. Med. Chem.* 17 (2009) 2623–2631.
- [40] H. Ohtsu, Z. Xiao, J. Ishida, M. Nagai, H.K. Wang, H. Itokawa, C.Y. Su, C. Shih, T. Chiang, E. Chang, Y. Lee, M.Y. Tsai, C. Chang, K.H. Lee, Antitumor agents. 217. Curcumin analogues as novel androgen receptor antagonists with potential as anti-prostate cancer agents, *J. Med. Chem.* 45 (2002) 5037–5042.
- [41] J.R. Fuchs, B. Pandit, D. Bhasin, J.P. Etter, N. Regan, D. Abdelhamid, C. Li, J. Lin, P.-K. Li, Structure–activity relationship studies of curcumin analogues, *Bioorg. Med. Chem. Lett.* 19 (2009) 2065–2069.
- [42] M.J. Ryu, M. Cho, J.Y. Song, Y.S. Yun, I.W. Choi, D.E. Kim, B.S. Park, S. Oh, Natural derivatives of curcumin attenuate the Wnt/beta-catenin pathway through down-regulation of the transcriptional coactivator p300, *Biochem. Biophys. Res. Commun.* 377 (2008) 1304–1308.
- [43] P. Anand, A.B. Kunnumakkara, R.A. Newman, B.B. Aggarwal, Bioavailability of curcumin: problems and promises, *Mol. Pharmacol.* 4 (2007) 807–818.
- [44] K.L. Kirk, Selective fluorination in drug design and development: an overview of biochemical rationales, *Curr. Top. Med. Chem.* 6 (2006) 1447–1456.
- [45] X. Li, T. Ohtsuki, T. Koyano, T. Kowithayakorn, M. Ishibashi, New Wnt/beta-catenin signaling inhibitors isolated from *Eleutherine palmifolia*, *Chem. Asian J.* 4 (2009) 540–547.
- [46] P. Polakis, Wnt signaling and cancer, *Genes Dev.* 14 (2000) 1837–1851.
- [47] C.R. Dass, E.T. Ek, K.G. Contreras, P.F. Choong, A novel orthotopic murine model provides insights into cellular and molecular characteristics contributing to human osteosarcoma, *Clin. Exp. Metastasis* 23 (2006) 367–380.
- [48] X. Qiu, Z. Liu, W.Y. Shao, X. Liu, D.P. Jing, Y.J. Yu, L.K. An, S.L. Huang, X.Z. Bu, Z.S. Huang, L.Q. Gu, Synthesis and evaluation of curcumin analogues as potential thioredoxin reductase inhibitors, *Bioorg. Med. Chem.* 16 (2008) 8035–8041.
- [49] G. Liang, S. Yang, L. Jiang, Y. Zhao, L. Shao, J. Xiao, F. Ye, Y. Li, X. Li, Synthesis and anti-bacterial properties of mono-carbonyl analogues of curcumin, *Chem. Pharm. Bull. (Tokyo)* 56 (2008) 162–167.